Because the Δd terms in the numerator and denominator of the right side of the equation (9.19) cancel, as do the negative signs before each term, equation (9.19) when combined with equation (9.13) yields

$$\text{Ratio} = R_{OS} = \frac{\alpha_A(\lambda_R)}{\alpha_A(\lambda_{IR})} = \frac{\ln\left(\dfrac{R_L}{R_H}\right)}{\ln\left(\dfrac{IR_L}{IR_H}\right)}. \tag{9.20}$$

Thus, by measuring the minimum and the maximum emergent light intensities of both the red and infrared wavelengths (R_L, R_H, IR_L, IR_H), a value for the term R_{OS} can be computed. Empirically derived calibration curves are then used to determine the oxygen saturation based on R_{OS}.

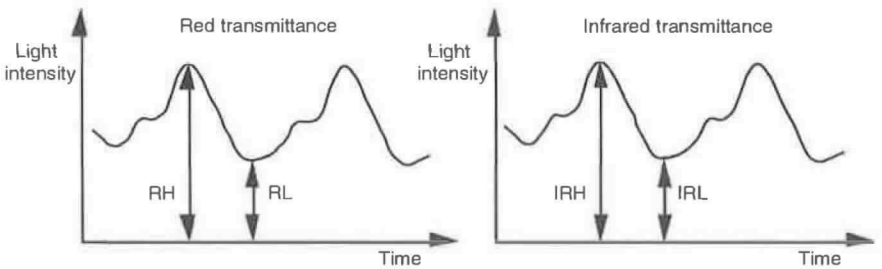

Figure 9.2. A graphical plot of transmitted light intensity converted into voltage. High (H) and low (L) signals are shown as a function of time of the transmittance of red (R) and infrared (IR) light through the finger.

9.3.2 Derivative method: noise reduction software

Yorkey (1996) derives the Ratio of Ratios by calculating using the separated AC and DC components of the measured signal. This mathematical derivation of the ratio of ratios is performed using the Beer–Lambert equation.

$$I_1 = I_0 \, e^{-\alpha L} \tag{9.21}$$

where I_1 is the emerging light intensity, I_0 is the incident light intensity, α is the relative extinction coefficient of the material and L is the path length. In this method, the Ratio of Ratios is determined using the derivatives. Assuming the change in path length is the same for both wavelengths during the same time interval between samples, the instantaneous change in path length (dL/dt) must also be the same for both wavelengths.

We can extend the general case of taking the derivative of e^u to our case

$$\frac{de^u}{dt} = e^u \frac{du}{dt} \tag{9.22}$$

MASIMO 2053
Apple v. Masimo
IPR2022-01300
APL_MAS_ITC_00015764
RX-0035.0147

$$\frac{dI_1}{dt} = I_0 e^{-\alpha L}\left(-\alpha \frac{dL}{dt}\right) \tag{9.23}$$

Therefore,

$$\frac{(dI_1/dt)}{I_1} = -\alpha \frac{dL}{dt}. \tag{9.24}$$

Here, I_1 is equal to the combined AC and DC component of the waveform and dI_1/dt is equal to the derivative of the AC component of the waveform. Using two wavelengths we have

$$\text{R of R} = \frac{(dI_R/dt)/I_R}{(dI_{IR}/dt)/I_{IR}} = \frac{-\alpha(\lambda_R)}{-\alpha(\lambda_{IR})}. \tag{9.25}$$

Instead of using the previous method of calculating the Ratio of Ratios based on the natural logarithm of the peak and valley values of the red and infrared signals, the value of the R of R can be calculated based on the derivative value of the AC component of the waveform.

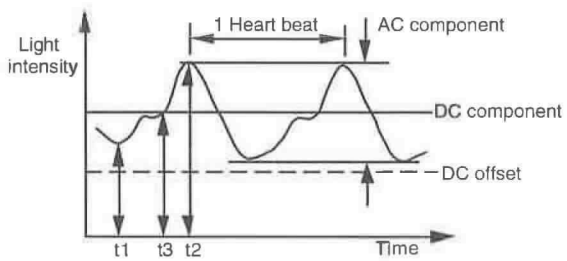

Figure 9.3. A waveform of the transmitted light intensity through a finger showing the AC component, the DC component and the DC offset.

Note in discrete time

$$\frac{dI_R(t)}{dt} \approx I_R(t_2) - I_R(t_1). \tag{9.26}$$

If we choose t_2 and t_1 to be the maximum and minimum of the waveform, we can refer to this difference as the AC value, and the denominator above evaluated at some point in time t_3 in between t_2 and t_1 as the DC value. So,

$$\frac{\dfrac{dI_R(t)/dt}{I_R}}{\dfrac{dI_{IR}(t)/dt}{I_{IR}}} \approx \frac{I_R(t_2) - I_R(t_1)}{I_R(t_3)} \Big/ \frac{I_{IR}(t_2) - I_{IR}(t_1)}{I_{IR}(t_3)} = \frac{AC_R}{DC_R} \Big/ \frac{AC_{IR}}{DC_{IR}} = R. \tag{9.27}$$

MASIMO 2053
Apple v. Masimo
IPR2022-01300
APL_MAS_ITC_00015765
RX-0035.0148

Potratz (1994) implemented another improved method for noise reduction called the derivative method of calculating the Ratio of Ratios. To calculate the Ratio of Ratios based on the derivative formula, a large number of sampled points along the waveform are used instead of merely the peak and valley measurements. A series of sample points from the digitized AC and AC + DC values for the infrared and red signals are used to form each data point. A digital FIR filtering step essentially averages these samples to give a data point. A large number of data points are determined in each period. The period is determined after the fact by noting where the peak and valley occur (figure 9.3).

From the AC signal, a derivative is then calculated for each pair of data points and used to determine the ratio of the derivatives for R and IR. A plot of these ratios over a period will ideally result in a straight line. Noise from the motion artifact and other sources will vary some values. But by doing the linear regression, a best line through a period can be determined, and used to calculate the Ratio of Ratios.

A problem with other systems was DC drift. Therefore, a linear extrapolation was performed between two consecutive negative peaks of the waveform. This adjusts the negative peak of the waveform as if the shift due to the system noise did not occur. A similar correction can be calculated using the derivative form of the waveform. In performing the correction of the DC component of the waveform, it is assumed that the drift caused by noise in the system is much slower than the waveform pulses and the drift is linear. The linear change on top of the waveform can be described by the function

$$g(t) = f(t) + mt + b \tag{9.28}$$

where m is equal to the slope of the waveform and b is equal to a constant.

The linear change added to the waveform does not affect the instantaneous DC component of the waveform. However, the derivative of the linear change will have an offset due to the slope of the interfering signal:

$$\mathrm{d}(f(t) + mt + b)/\mathrm{d}t = \mathrm{d}f(t)/\mathrm{d}t + m. \tag{9.29}$$

if we assume that the offset is constant over the period of time interval, then the Ratio of Ratios may be calculated by subtracting the offsets and dividing:

$$\text{R of R} = \frac{Y}{X} = \frac{(y - m_y)}{(x - m_x)} \tag{9.30}$$

where y and x are the original values and m_x and m_y are the offsets.

Since the Ratio of Ratios is constant over this short time interval the above formula can be written as

$$\frac{(y - m_y)}{(x - m_x)} = R. \tag{9.31}$$

Therefore,

$$y = Rx - Rm_x + m_y. \tag{9.32}$$

Since it was assumed that m_1, m_2, and R are constant over the time interval, we have an equation in the form of $y = mx + b$ where m is the Ratio of Ratios. Thus,

MASIMO 2053
Apple v. Masimo APL_MAS_ITC_00015766
IPR2022-01300
RX-0035.0149

we do a large number of calculations of the Ratio of Ratios for each period, and then do the best fit calculation to the line $y = Rx + b$ to fit the optimum value of R for that period, taking into account the constant b which is caused by DC drift.

To determine the Ratio of Ratios exclusive of the DC offset we do a linear regression. It is preferred to take points along the curve having a large differential component, for example, from peak to valley. This will cause the mx term to dominate the constant b:

$$R = \frac{n\sum x_j y_j - \sum x_j \sum y_j}{n\sum x_j{}^2 - (\sum x_j)^2} \tag{9.33}$$

where n = # of samples, j = sample #, $x = I_R \, dI_{IR} / dt$, $y = I_{IR} \, dI_R / dt$.

Prior sampling methods typically calculate the Ratio of Ratios by sampling the combined AC and DC components of the waveform at the peak and valley measurements of the waveform. Sampling a large number of points on the waveform, using the derivative and performing a linear regression increases the accuracy of the Ratio of Ratios, since noise is averaged out. The derivative form eliminates the need to calculate the logarithm. Furthermore doing a linear regression over the sample points not only eliminates the noise caused by patient movement of the oximeter, it also decreases waveform noise caused by other sources.

9.4 GENERAL PROCESSING STEPS OF OXIMETRY SIGNALS

The determination of the Ratio of Ratios (R_{OS}) requires an accurate measure of both the baseline and pulsatile signal components (Frick *et al* 1989). The baseline component approximates the intensity of light received at the detector when only the fixed nonpulsatile absorptive component is present in the finger. This component of the signal is relatively constant over short intervals and does not vary with nonpulsatile physiological changes, such as movement of the probe. Over a relatively long time, this baseline component may vary significantly. The magnitude of the baseline component at a given point in time is approximately equal to the level identified as R_H (figure 9.2). However, for convenience, the baseline component may be thought of as the level indicated by R_L, with the pulsatile component varying between the values of R_H and R_L over a given pulse. Typically, the pulsatile component may be relatively small in comparison to the baseline component and is shown out of proportion in figure 9.3. Because the pulsatile components are smaller, greater care must be exercised with respect to the measurement of these components. If the entire signal, including the baseline and the pulsatile components, were amplified and converted to a digital format for use by microcomputer, a great deal of the accuracy of the conversion would be wasted because a substantial portion of the resolution would be used to measure the baseline component (Cheung *et al* 1989).

In this process, a substantial portion of the baseline component termed offset voltage V_{OS} is subtracted off the input signal V_1. The remaining pulsatile component is amplified and digitized using an ADC. A digital reconstruction is then produced by reversing the process, wherein the digitally provided information allows the gain to be removed and the offset voltage added back.

MASIMO 2053
Apple v. Masimo
IPR2022-01300
APL_MAS_ITC_00015767
RX-0035.0150

This step is necessary because the entire signal, including the baseline and pulsatile components is used in the oxygen saturation measurement process.

Feedback from the microcomputer is required to maintain the values for driver currents I_0, V_{os} and gain A at levels appropriate to produce optimal ADC resolution (figure 9.4). Threshold levels L1 and L2 slightly below and above the maximum positive and negative excursions L3 and L4 allowable for the ADC input are established and monitored by the microcomputer (figure 9.5). When the magnitude of the input to and output from the ADC exceeds either of the thresholds L1 or L2, the drive currents I_D are adjusted to increase or decrease the intensity of light impinging on the detector. This way, the ADC is not overdriven and the margin between L1 and L3 and between L2 and L4 helps assure this even for rapidly varying signals. An operable voltage margin for the ADC exists outside of the thresholds, allowing the ADC to continue operating while the appropriate feedback adjustments to A and V_{os} are made. When the output from the ADC exceeds the positive and negative thresholds L5 or L6, the microcomputer responds by signaling the programmable subtractor to increase or decrease the voltage V_{os} being subtracted. This is accomplished based on the level of the signal received from the ADC. Gain control is also established by the microcomputer in response to the output of the ADC (Cheung *et al* 1989).

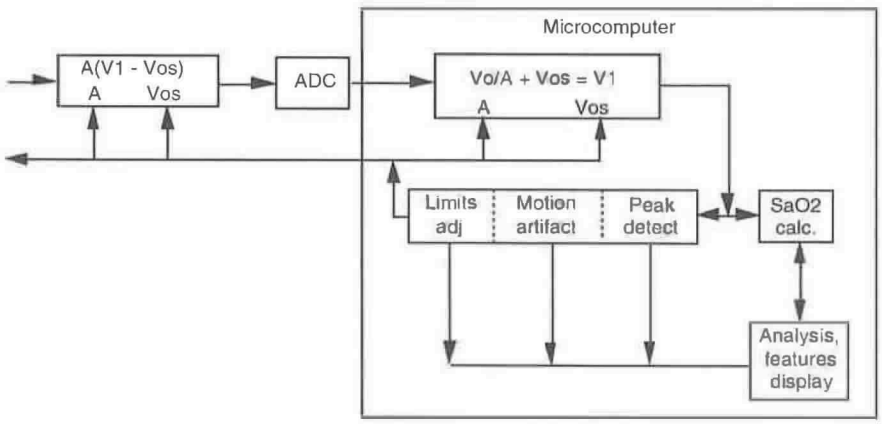

Figure 9.4. A functional block diagram of the microcomputer feedback illustrating the basic operation of the feedback control system. The DC value of the signal is subtracted before digitizing the waveform to increase the dynamic range of conversion. The removed DC value is later added to the digitized values for further signal processing (Cheung *et al* 1989).

A program of instructions executed by the Central Processing Unit of the microcomputer defines the manner in which the microcomputer provides servosensor control as well as produces measurements for display. The first segment of the software is the interrupt level routine.

9.4.1 Start up software.

The interrupt level routine employs a number of subroutines controlling various portions of the oximeter. At the start up, calibration of the oximeter is

MASIMO 2053
Apple v. Masimo APL_MAS_ITC_00015768
IPR2022-01300
RX-0035.0151

performed. After calibration, period zero subroutine is executed which includes five states, zero through four (figure 9.6).

Period zero subroutine is responsible for normal sampling

State 0: Initialize parameters
State 1: Set drive current
State 2: Set offsets
State 3: Set gains
State 4: Normal data acquisition state.

Probe set-up operations are performed during the states zero to three of this subroutine. During these states probe parameters including the amplifier gain A and offset voltage V_{os} are initialized, provided that a finger is present in the probe. State 4 of the interrupt period zero subroutine is the normal data acquisition state. The signals produced in response to light at each wavelength are then compared with the desired operating ranges to determine whether modifications of the driver currents and voltage offsets are required. Finally state 4 of the period zero subroutine updates the displays of the oximeter. Sequential processing returns to state 0 whenever the conditions required for a particular state are violated (Cheung *et al* 1989).

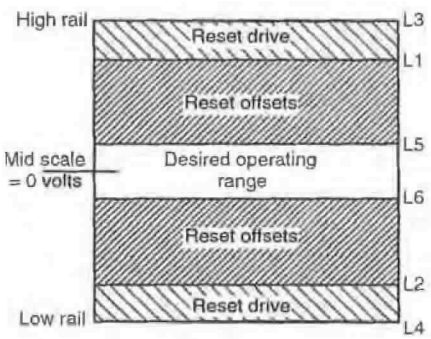

Figure 9.5 A graphical representation of the possible ranges of digitized signal, showing the desired response of the I/O circuit and microcomputer at each of the various possible ranges (Cheung *et al* 1989).

9.5 TRANSIENT CONDITIONS

The relative oxygen content of a patient's arterial pulses and the average background absorbance remain about the same from pulse to pulse. Therefore, the red and infrared light that is transmitted through the pulsatile flow produces a regularly modulated waveform with periodic pulses of comparable shape and amplitude and a steady state background transmittance. This regularity in shape helps in accurate determination of the oxygen saturation of the blood based on the maximum and minimum transmittance of the red and infrared light.

Changes in a patient's local blood volume at the probe site due to motion artifact or ventilatory artifact affect the absorbance of light. These localized

MASIMO 2053
Apple v. Masimo
IPR2022-01300
APL_MAS_ITC_00015769
RX-0035.0152

changes often introduce artificial pulses into the blood flow causing the periodic pulses ride on a background intensity component of transmittance that varies as blood volume changes. This background intensity component variation, which is not necessarily related to changes in saturation, affects the pulse to pulse uniformity of shape, amplitude and expected ratio of the maximum to minimum transmittance, and can affect the reliability and accuracy of oxygen saturation determination (Stone and Briggs 1992).

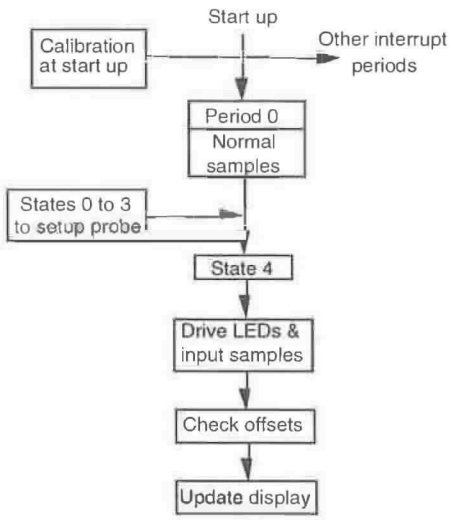

Figure 9.6. Flow chart of a portion of an interrupt level software routine included in the microcomputer (Cheung *et al* 1989).

In addition, there are times when the patient's background level of oxygen saturation undergoes transient changes, for example, when the patient loses or requires oxygen exchange in the lungs while under gaseous anesthesia. The transient waveform distorts the pulse shape, amplitude, and the expected ratio of the pulses, which in turn affects the reliability and accuracy of the oxygen saturation determination.

With changes in the background intensity absorbance component due to artifacts from changes in blood volume or transient saturation changes, the determined saturation value is not accurate and it would not become accurate again until the average absorbance level stabilizes.

The saturation calculations based upon transient signals provide an overestimation or underestimation of the actual saturation value, depending upon the trend. The transmittance of red light increases as oxygen saturation increases resulting in a signal value having a smaller pulse, and the transmittance of the infrared light decreases as saturation increases resulting in the infrared pulsatile amplitude increasing. For these wavelengths, the transmittance changes with saturation are linear in the range of clinical interest, i.e., oxygen saturation between 50% and 100%. The accuracy of the estimation is of particular concern during rapid desaturation. In such a case, the determined saturation based on the

MASIMO 2053
Apple v. Masimo
IPR2022-01300
APL_MAS_ITC_00015770
RX-0035.0153

detected signals indicates a greater drop than the actual value. This underestimation of oxygen saturation may actuate low limit saturation alarms that can result in inappropriate clinical decisions.

The pulsatile amplitude is usually quite small, typically less than 5% of the overall intensity change and any small change in overall or background transmittance, such as slight changes in average blood saturation, can have a relatively large effect on the difference in maximum and minimum intensity of the light levels. Because the change in transmittance with changing oxygen saturation is opposite in direction for the red and infrared, this can result in overestimation of the pulsatile ratio during periods when saturation is decreasing, and underestimation during periods when saturation is increasing. It is therefore essential to compensate for the effects of transient conditions and localized blood volume changes on the actual signal, thereby providing a more accurate estimation of the actual oxygen saturation value.

This can be achieved by using a determined rate of change from pulse to pulse, using interpolation techniques and by using the low frequency characteristics of the detected signal values.

The transient error is corrected by linear interpolation where the determined maxima and minima for a first and second optical pulses are obtained, the second pulse following the first. The respective rates of change in the transmittance due to the transient are determined from the maximum transmittance point of the first detected pulse to the second detected pulse (Stone and Briggs 1992). The determined rates of change are then used to compensate any distortion in the detected transmittance of the first detected pulse introduced by the transient in accordance with the following algorithm

$$V_{\max}(n)^{*} = V_{\max}(n) + [V_{\max}(n) - V_{\max}(n+1)] \times \frac{[t_{\max}(n) - t_{\min}(n)]}{[t_{\max}(n+1) - t_{\max}(n)]} \quad (9.34)$$

where $t_{\max}(n)$ is the time of occurrence of the detected maximum transmittance at the n maximum, $t_{\min}(n)$ is the time of occurrence of the detected minimum transmittance of the wavelength at the n minimum, $V_{\max}(n)$ is the detected optical signal maximum value at the maximum transmittance of the wavelength at the n maximum $V_{\max}(n)^{*}$ is the corrected value, for n being the first optical pulse, and $n + 1$ being the second optical pulse of that wavelength.

By application of the foregoing linear interpolation routine, the detected maximum transmittance value at $t_{\max}(n)$ can be corrected, using the values $t_{\max}(n+1)$, detected at the next coming pulse, to correspond to the transmittance value that would be detected as if the pulse were at steady state conditions. The corrected maximum value and the detected (uncorrected) minimum value thus provide an adjusted optical pulse maximum and minimum that correspond more closely to the actual oxygen saturation in the patient's blood at that time, not withstanding the transient condition. Thus, using the adjusted pulse values in place of the detected pulse values in the modulation ratio for calculating oxygen saturation provides a more accurate measure of oxygen saturation than would otherwise be obtained during transient operation.

Similarly, the respective rates of change in the transmittance are determined from the minimum transmittance point of the first detected pulse to the minimum of the second detected pulse. The determined rates of change are then used to compensate for any distortion in the detected minimum transmittance of the

MASIMO 2053
Apple v. Masimo
IPR2022-01300
APL_MAS_ITC_00015771
RX-0035.0154

second detected pulse introduced by the transient in accordance with the following algorithm

$$V_{\min}(n)^{*} = V_{\min}(n-1) + [V_{\min}(n) - V_{\min}(n-1)] \times \frac{[t_{\max}(n) - t_{\min}(n-1)]}{[t_{\min}(n) - t_{\min}(n-1)]} \quad (9.35)$$

where $t_{\max}(n)$ is the time of occurrence of the detected maximum transmittance at the n maximum; $t_{\min}(n)$ is the time of occurrence of the detected minimum transmittance of the wavelength at the n minimum; $V_{\min}(n)$ is the detected optical signal minimum value at the minimum transmittance of the wavelength at the n minimum; $V_{\min}(n)^{*}$ is the corrected value, for n being the second optical pulse, and $n-1$ being the first optical pulse of that wavelength.

By application of the foregoing linear interpolation routine, the detected minimum transmittance value at $t = n$ can be compensated using the detected values at the preceding pulse $t = n - 1$, to correspond to the transmittance value that would be detected as if the pulse were detected at steady state conditions. The compensated minimum value and the detected (uncompensated) maximum value thus provide an adjusted optical pulse maximum and minimum that correspond more closely to the actual oxygen saturation in the patient's blood at that time, notwithstanding the transient condition. Thus, using the adjusted pulse values in place of the detected pulse values in the modulation ratio for calculating oxygen saturation provides a more accurate measure of oxygen saturation than would otherwise be obtained during transient operation.

As is apparent from the algorithms, during steady state conditions the compensated value is equal to the detected value. Therefore, the linear interpolation routine may be applied to the detected signal at all times, rather than only when transient conditions are detected. Also, the algorithm may be applied to compensate the detected minimum or maximum transmittance values by appropriate adjustment of the algorithm terms. The amount of oxygen saturation can then be determined from this adjusted optical pulse signal by determining the relative maxima and minima as compensated for the respective wavelengths and using that information in determining the modulation ratios of the known Lambert–Beer equation.

The Nellcor® N-200 oximeter is designed to determine the oxygen saturation in one of the two modes. In the unintegrated mode the oxygen saturation determination is made on the basis of optical pulses in accordance with conventional pulse detection techniques. In the ECG synchronization mode the determination is based on enhanced periodic data obtained by processing the detected optical signal and the ECG waveform of the patient.

The calculation of saturation is based on detecting maximum and minimum transmittance of two or more wavelengths whether the determination is made pulse by pulse (the unintegrated mode) or based on an averaged pulse that is updated with the occurrence of additional pulses to reflect the patient's actual condition (the ECG synchronized mode).

Interrupt programs control the collection and digitization of incoming optical signal data. As particular events occur, various software flags are raised which transfer operation to various routines that are called from a main loop processing routine.

The detected optical signal waveform is sampled at a rate of 57 samples per second. When the digitized red and infrared signals for a given portion of

MASIMO 2053
Apple v. Masimo
IPR2022-01300
APL_MAS_ITC_00015772
RX-0035.0155

detected optical signals are obtained, they are stored in a buffer called DATBUF and a software flag indicating the presence of data is set. This set flag calls a routine called MUNCH, which processes each new digitized optical signal waveform sample to identify pairs of maximum and minimum amplitudes corresponding to a pulse. The MUNCH routine first queries whether or not there is ECG synchronization, then the MUNCH routine obtains the enhanced composite pulse data in the ECG synchronization mode. Otherwise, MUNCH obtains the red and infrared optical signal sample stored in DATBUF, in the unintegrated mode. The determined maximum and minimum pairs are then sent to a processing routine for processing the pairs. Preferably, conventional techniques are used for evaluating whether a detected pulse pair is acceptable for processing as an arterial pulse and performing the saturation calculation, whether the pulse pair is obtained from the DATBUF or from the enhanced composite pulse data.

The MUNCH routine takes the first incoming pulse data and determines the maximum and minimum transmittance for each of the red and infrared detected optical signals, and then takes the second incoming pulse data, and determines the relative maximum and minimum transmittance. The routine for processing the pairs applies the aforementioned algorithm to the first and second pulse data of each wavelength. Then the oxygen saturation can be determined using the corrected minimum and detected maximum transmittance for the second pulses of the red and infrared optical signals. Some of the examples demonstrate the above application.

Example 1

Figure 9.7(*a*) shows the representative plethysmographic waveforms in a steady state condition for the red and infrared detected signals. $V_{max}R(1)$ equals 1.01 V, and $V_{min}R(1)$ equals 1.00 V, for $n = 1$, 2 and 3 pulses. $V_{min}R(n)$ is the detected optical signal minimum value at the minimum transmittance at the n pulse minimum. The modulation ratio for the maxima and minima red signal is:

$$\frac{V_{max}R(n)}{V_{min}R(n)} = \frac{1.01v}{1.00v} = 1.01.$$

For the infrared wavelength, $V_{max}IR(n)$ equals 1.01 V and $V_{min}IR(n)$ equals 1.00 V and the determined modulation ratio is 1.01.

Using these determined modulation ratios in the formula for calculating the ratio R provides:

$$R = \frac{\ln[V_{max}R(n)/V_{min}R(n)]}{\ln[V_{max}IR(n)/V_{min}IR(n)]} = \frac{0.01}{0.01} = 1.00.$$

A calculated $R = 1$ corresponds to an actual saturation value of about 81% when incorporated into the saturation equation. A saturation of 81% corresponds to a healthy patient experiencing a degree of hypoxia for which some corrective action would be taken.

MASIMO 2053
Apple v. Masimo
IPR2022-01300
APL_MAS_ITC_00015773
RX-0035.0156

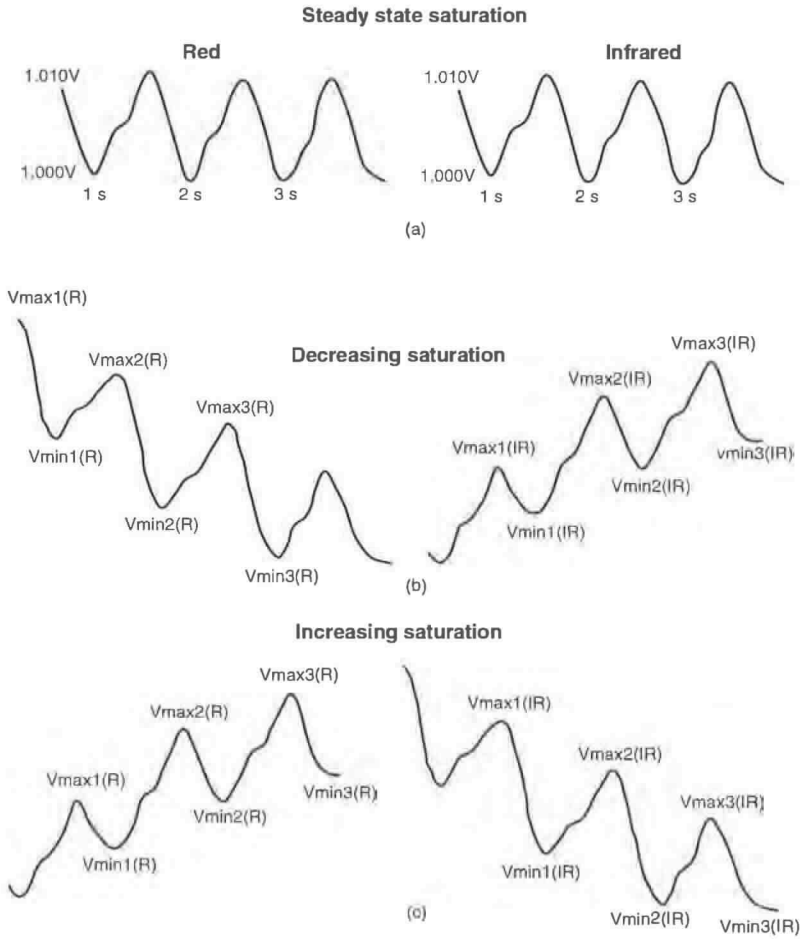

Figure 9.7. Graphical representation of detected optical signals during the steady state and transient conditions (Stone and Briggs 1992).

Example 2

Figure 9.7(*b*) shows the representative plethysmographic waveforms for a patient during desaturation or decreasing saturation transient conditions for the red and infrared detected signals having optical pulses $n = 1$, 2, and 3. However, in this transient example, it is known at $n = 1$, that the actual saturation of the patient is very close to that during the steady state conditions in example 1. In this transient example, the detected values are as follows for both the red and infrared signals:

MASIMO 2053
Apple v. Masimo
IPR2022-01300
APL_MAS_ITC_00015774
RX-0035.0157

$t_{max}(1) = 1.0$ s	$V_{max}R(1) = 1.012$ V	$V_{max}IR(1) = 1.008$ V
$t_{min}(1) = 1.2$ s	$V_{min}R(1) = 1.000$ V	$V_{min}IR(1) = 1.000$ V
$t_{max}(2) = 2.0$ s	$V_{max}R(2) = 1.002$ V	$V_{max}IR(2) = 1.018$ V
$t_{min}(2) = 2.2$ s	$V_{min}R(2) = 0.990$ V	$V_{min}IR(2) = 1.010$ V
$t_{max}(3) = 3.0$ s	$V_{max}R(3) = 0.992$ V	$V_{max}IR(3) = 1.028$ V
$t_{min}(3) = 3.2$ s	$V_{min}R(3) = 0.980$ V	$V_{min}IR(3) = 1.020$ V

Calculating the oxygen saturation ratio R at $n = 1$, using the detected optical signal provides the following

$$\begin{aligned} R &= \frac{\ln[V_{max}R(1)/V_{min}R(1)]}{\ln[V_{max}IR(1)/V_{min}IR(1)]} \\ &= \ln[1.012/1.000]/\ln[1.008/1.000] \\ &= \ln[1.012]/\ln[1.008] \\ &= 0.012/0.008 \quad = 1.5. \end{aligned}$$

The calculated saturation ratio of 1.5 based on the detected transmittance corresponds to a calculated oxygen saturation of about 65 for the patient, which corresponds to severe hypoxia in an otherwise healthy patient. This contrasts with the known saturation of about 81% and demonstrates the magnitude of the underestimation of the oxygen saturation (overestimation of desaturation) due to the distortion in transmittance of the red and infrared light caused by transient conditions.

Applying the correction algorithm to correct the distorted maximum transmittance point of the detected red signal during the transient condition:

$$\begin{aligned} V_{max}R(1)^{*} &= V_{max}R(1) - [V_{max}R(1) - V_{max}R(2)] \times \frac{[t_{max}(1) - t_{min}(1)]}{[t_{max}(2) - t_{max}(1)]} \\ &= 1.012 - [1.012 - 1.002] \times [1.0 - 1.2]/[1.0 - 2.0] \\ &= 1.010. \end{aligned}$$

and correspondingly for the maximum transmittance of the detected infrared signal

$$\begin{aligned} V_{max}IR(1)^{*} &= 1.008 - [1.008 - 1.018] \times [1.0 - 1.2]/[1.0 - 2.0] \\ &= 1.010 \end{aligned}$$

Thus, by replacing $V_{max}R(n)$ with $V_{max}R(n)^{*}$ and replacing $V_{max}IR(n)$ with $V_{max}IR(n)^{*}$ in the calculations for determining the oxygen saturation ratio R, we have

$$\begin{aligned} R &= \frac{\ln[V_{max}R(1)^{*}/V_{min}R(1)]}{\ln[V_{max}IR(1)^{*}/V_{min}IR(1)]} \\ &= \ln[1.010/1.00]/\ln[1.010/1.00] \\ &= 0.01/0.01 \\ &= 1.0. \end{aligned}$$

MASIMO 2053
Apple v. Masimo
IPR2022-01300
APL_MAS_ITC_00015775
RX-0035.0158

Thus, basing the saturation calculations on the corrected maximum transmittance values and the detected minimum transmittance values, the corrected R value corresponds to the same R for the steady state conditions and the actual oxygen saturation of the patient.

Example 3

Figure 9.7(*c*) shows the representative plethysmographic waveforms for a patient during desaturation or decreasing saturation transient conditions for the red and infrared detected signals having optical pulses $n = 1$, 2 and 3. However, in this transient example, it is known that at $n = 2$, the actual saturation of the patient is very close to that during the steady state conditions in example 1. In this transient example, the detected values are as follows for both the red and infrared signals:

$t_{max}(1) = 1.0$ s	$V_{max}R(1) = 1.022$ V	$V_{max}IR(1) = 1.002$ V
$t_{min}(1) = 1.2$ s	$V_{min}R(1) = 1.008$ V	$V_{min}IR(1) = 0.992$ V
$t_{max}(2) = 2.0$ s	$V_{max}R(2) = 1.012$ V	$V_{max}IR(2) = 1.012$ V
$t_{min}(2) = 2.2$ s	$V_{min}R(2) = 0.998$ V	$V_{min}IR(2) = 1.002$ V
$t_{max}(3) = 3.0$ s	$V_{max}R(3) = 1.002$ V	$V_{max}IR(3) = 1.022$ V
$t_{min}(3) = 3.2$ s	$V_{min}R(3) = 0.988$ V	$V_{min}IR(3) = 1.012$ V

Calculating the oxygen saturation ratio R at $n = 2$, using the detected optical signal provides the following

$$R = \frac{\ln[V_{max}R(2)/V_{min}R(2)]}{\ln[V_{max}IR(2)/V_{min}IR(2)]}$$
$$= \ln[1.012/0.998]/\ln[1.012/1.002]$$
$$= 0.01393/0.0099 \quad = 1.4.$$

Thus, the calculated saturation ratio of 1.4 based on the detected transmittance corresponds to a calculated oxygen saturation of about 51% for the patient, which corresponds to severe hypoxia in an otherwise healthy patient. This contrasts with the known saturation of about 81% and demonstrates the magnitude of the underestimation of the oxygen saturation (overestimation of desaturation) due to the distortion in transmittance of the red and infrared light caused by transient conditions.

Applying the correction algorithm to correct the distorted minimum transmittance point of the detected red signal during the transient condition, we find the following:

$$V_{min}R(2)^* = V_{min}R(2) - [V_{min}R(2) - V_{min}R(1)] \times \frac{[t_{max}(2) - t_{min}(1)]}{[t_{min}(2) - t_{max}(1)]}$$
$$= 1.008 - [0.998 - 1.008] \times [2.0 - 1.2]/[2.2 - 1.2]$$
$$= 1.0$$

and correspondingly for the minimum transmittance of the detected infrared optical signal we have:

MASIMO 2053
Apple v. Masimo
IPR2022-01300
APL_MAS_ITC_00015776
RX-0035.0159

$$V_{\min}\mathrm{IR}(2)^{*} = 0.992 - [1.002 - 0.992] \times 0.8$$
$$= 1.0.$$

Thus, by replacing $V_{\min}\mathrm{R}(n)$ with $V_{\min}\mathrm{R}(n)^{*}$ and replacing $V_{\min}\mathrm{IR}(n)$ with $V_{\min}\mathrm{IR}(n)^{*}$ in the calculations for determining oxygen saturation ratio R we have:

$$R = \frac{\ln[V_{\max}\mathrm{R}(2) / V_{\min}\mathrm{R}(2)^{*}]}{\ln[V_{\max}\mathrm{IR}(2) / V_{\min}\mathrm{IR}(2)^{*}]}$$
$$= \ln[1.012 / 1.0] / \ln[1.012 / 1.0]$$
$$= 1.0.$$

Thus, basing the saturation calculations on the corrected minimum transmittance values and the detected maximum transmittance values, the corrected R value corresponds to the same R for the steady state conditions and the actual oxygen saturation of the patient.

9.6 ECG SYNCHRONIZATION ALGORITHMS

Electrical heart activity occurs simultaneously with the heartbeat and can be monitored externally and characterized by the electrocardiogram waveform. The ECG waveform comprises a complex waveform having several components that correspond to electrical heart activity of which the QRS component relates to ventricular heart contraction. The R wave portion of the QRS component is typically the steepest wave therein having the largest amplitude and slope, and may be used for indicating the onset of cardiac activity. The arterial blood pulse flows mechanically and its appearance in any part of the body typically follows the R wave of the electrical heart activity by a determinable period of time. This fact is utilized in commercially available pulse oximeters to enhance their performance. Another advantage of recording ECG is that it provides a redundancy in calculating the heart rate from both the ECG signal and the optical signal to continuously monitor the patient even if one of the signals is lost (figure 9.8).

With ECG synchronization, the pulse oximeter uses the electrocardiographic (ECG) QRS complex as a timing indicator that the optical pulse will soon appear at the probe site. The R portion of the ECG signal is detected and the time delay by which an arterial pulse follows the R wave is determined to establish a time window an arterial pulse is to be expected. By using the QRS complex to time the oximeter's analysis of the optical pulse signal, ECG processing synchronizes the analysis of oxygen saturation and pulse rate data. The established time window provides the oximeter with a parameter enabling the oximeter to analyze the blood flow only when it is likely to have a pulse present for analysis. This method of signal processing passes those components of the signal that are coupled to the ECG (i.e., the peripheral pulse), while attenuating those components that are random with respect to the ECG (e.g., motion artifact or other noise in the signal).

MASIMO 2053
Apple v. Masimo
IPR2022-01300
APL_MAS_ITC_00015777
RX-0035.0160

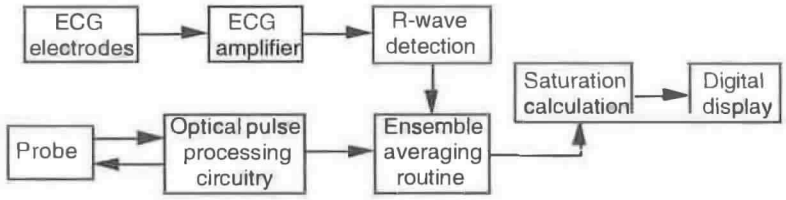

Figure 9.8. Block diagram illustrating the ECG processing components, its subcomponents and their relationship in an oximeter.

9.6.1 Nellcor® system

C-LOCK ECG synchronization enhances the signal-processing capabilities of Nellcor® systems such as the N-200 pulse oximeter and the N-1000 multifunction monitor. This improves the quality of the optical signal in certain clinical settings in which the performance of a conventional pulse oximeter may deteriorate, e.g. when a patient is moving or has poor peripheral pulses. Consequently, C-LOCK signal processing extends the range of clinical situations in which pulse oximetry may be used. Patient movement and poor peripheral pulses present similar problems for a conventional pulse oximeter: performance may deteriorate because the oximeter is unable to distinguish between the true optical pulse signal and background noise. C-LOCK ECG synchronization improves signal quality in these difficult signal-detection settings (Goodman and Corenman 1990).

The digital optical signal is processed by the microprocessor of the Nellcor N-1000 Pulse Oximeter in order to identify individual optical pulses and to compute the oxygen saturation from the ratio of maximum and minimum pulse levels as seen by the red wavelength compared to the pulse seen by the infrared wavelength.

Noninvasive pulse oximeters process optical signals which are prone to motion artifacts caused by the muscle movement proximate to the probe site. The spurious pulses induced in the optical signals may cause the pulse oximeter to process the artifact waveform and provide erroneous data. This problem is particularly significant with infants, fetuses, or patients that do not remain still during monitoring. Another problem exists in circumstances where the patient is in poor condition and the pulse strength is very weak. In continuously processing the optical data, it can be difficult to separate the true pulsatile component from the artifact pulses and noise because of low signal to noise ratio. Inability to reliably detect the pulsatile component in the pulsatile signal may result in a lack of the information needed to calculate oxygen blood saturation.

By incorporating the patient's heart activity into the pulse oximeter, problems due to motion artifact and low signal-to-noise ratio can be solved. Processing of the signals that occur during a period of time when the optical pulses are expected to be found, increases the likelihood that the oximeter will process only optical waveforms that contain the pulsatile component of arterial blood, and will not process spurious signals.

MASIMO 2053
Apple v. Masimo
IPR2022-01300
APL_MAS_ITC_00015778
RX-0035.0161

The software incorporated into the microprocessor for processing the ECG signals and displaying the calculated ECG pulse rate receives the digitized version of diagnostic ECG signal (DECG) and filtered ECG signals (FECG). The microprocessor calculates the amplitude of the ECG waveform and controls the AGC (automatic gain control) amplifier, so that DECG and FECG will fall within the voltage range limits of the electronic circuitry used to process these signals.

The microprocessor regularly searches a status input latch at a rate of 57 cycles per second. The output of detected R wave (DRW) sets the latch to a logical 1 when the R wave is detected. Depending on the status, the microprocessor selects the next operation and resets the DRW latch to 0. At this first level, the microprocessor counts the time interval beginning from the detection of an R wave pulse until the occurrence of the next logical 1 at the status input latch. Based on this time interval, the pulse oximeter displays the pulse rate. After averaging several time intervals and establishing a regular ECG pulse rate, the microprocessor will change to the second level of processing.

After the detection of an R wave pulse, the microprocessor separately analyzes the digital optical signal and correlates the period of time by which an optical pulse follows the detected R wave pulse to establish the time window during which the optical pulse is likely to occur. During this second level, the pulse oximeter just calculates and displays the time period or pulse rate between DRW pulses.

The third level of processing starts after a time window has been established. On detecting an R wave pulse, the microprocessor activates the time window so that only optical signals detected within the time window following the occurrence of an R wave pulse will be evaluated for acceptance or rejection and for use in calculating and displaying vital measurements such as oxygen saturation, pulse flow, and pulse rate. The evaluation of a detected pulse is made in conjunction with a preselected confidence factor that is associated with the quality of the optical signals. The higher the optical signal quality, the better the correlation between the recorded pulse history and the detected pulse, and the higher the confidence level. The confidence level may be set automatically by the microprocessor, or it may be adjusted by the operator. The microprocessor will reject any detected pulses occurring outside the time window. A typical time window for an adult male using a fingertip oximeter probe may be about 50 ms ±10 ms after the occurrence of an R wave. The oximeter will also reject any additional pulses detected after an optical pulse is detected within the same time window, even though the time window has not expired.

However, if the optical pulse is not found within an opened time window, the microprocessor will continue to search for optical pulses using the degraded criteria during the time window period for about three successive detected R wave (DRW) pulses, after which it continues to search with degraded criteria. After a specific interval, e.g. 10 s, without detecting an optical pulse, the microprocessor will revert to independent or nonintegrated processing of the optical and ECG signals, returning the pulse oximeter to startup conditions. Therefore, if the oximeter cannot establish or maintain a reliable correlation between the R wave and the optical pulse, the waveforms will be processed independently. The display will indicate whether the pulse oximeter is operating in integrated or nonintegrated mode. After attaining the third level of processing, losing either the ECG or optical pulse signals will activate an alarm and return the program to the startup condition.

MASIMO 2053
Apple v. Masimo APL_MAS_ITC_00015779
IPR2022-01300
RX-0035.0162

9.6.1.1 R-wave determination routine. The R-wave determination routine begins with electric signals received from the ECG leads and calculating the R–R period RRPER between the last detected R wave and the present R wave (figure 9.9). The average period HISTORY from the previous R waves and the present R wave is calculated and the determined RRPER is compared to the average period HISTORY (Goodman and Corenman 1990). If RRPER does not correspond to HISTORY, the R wave ECG flag is reset and the routine is exited to await another R wave. If RRPER does correspond to HISTORY, a timer is activated to measure the interval from the occurrence of the R wave to the occurrence of the optical pulse. Output HR (ECG heart rate) is calculated based on successive R waves. The system determines whether a series of R–R periods have been synchronized (ECG synchronization). If not synchronized, then the system checks for alarms by comparing output HR to a preselected heart rate and generates an alarm if the output HR is too low. If the ECG is synchronized but the optical pulse to optical pulse is not synchronized, the output HR is sent to the display and then checked for alarms. If the optical signal is synchronized, then the system just checks for alarms. Only if the ECG is synchronized, the optical pulse is not synchronized, and the R wave looks like a valid R wave by comparison with HISTORY, then HISTORY is updated using the new R wave. After updating HISTORY, the system itself is updated (TIME OUT) to maintain synchronization. If TIME OUT is not updated for a period of five seconds, then ECG synchronization is lost and the routine must begin building a new history.

9.6.1.2 The systems routine. The system routine for processing digital optical pulse information for optical pulses to send to LEVEL 3 is flow charted (figure 9.10). The system begins by continuously evaluating the data from the detected digital optical signal (Goodman and Corenman 1990). The data are first evaluated for compatibility with signal processing. If the data are over or undervalued electronically, i.e., beyond the voltage range of the circuitry, then the system exits the routine, and the LED intensities are adjusted to correct the electrical values accordingly. When the data are compatible, they are next evaluated for a maximum signal. A relative maximum is determined and saved. The next value is compared to the saved value, and if it is a new maximum, it is saved instead. When the value found is not a new maximum, then a MAX FLAG is set. Thereafter, the system evaluates the following data received, by passing the maximum value section, to find the maximum slope, again by successive comparisons. When the largest slope value is found, it is saved and the SLOPE FLAG is set. Thereafter, the following data are evaluated, by passing the maximum and slope calculations, to find the minimum value corresponding to the end of the pulse. When the smallest minimum is found, it is saved and the slope value that was saved is compared with a pre-established minimum threshold to determine whether it is large enough to be a possible optical pulse. If it is not large enough, then the pulse is rejected, the flags are reset, and the routine begins processing the next possible pulse. If the slope is large enough, then the pulse parameters, maximum, minimum, and slope, are saved in memory for use by LEVEL 3 processing in evaluating the possible pulse. Then, the time delay from the R wave to the possible pulse is calculated. Thereafter, the DATA FLAG is set indicating to LEVEL 3 that there is a possible pulse to be evaluated, the MAX and SLOPE FLAGs are reset, and the routine begins again to process the following data, looking for new maximum values corresponding to possible pulses.

MASIMO 2053
Apple v. Masimo APL_MAS_ITC_00015780
IPR2022-01300
RX-0035.0163

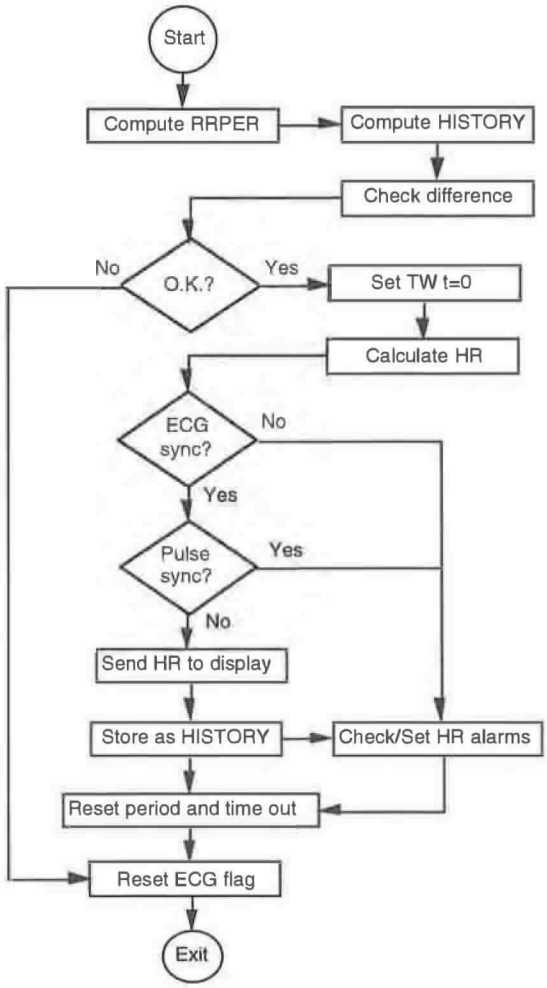

Figure 9.9. The R wave determination routine calculates RRPER, compares it with the average period HISTORY. If RRPER corresponds to HISTORY, the interval between the occurrence of R wave and occurrence of pulse is measured. The algorithm checks for ECG synchronization, alarms and displays heart rate (HR) (Goodman and Corenman 1990).

9.6.1.3 LEVEL 3 software. Figure 9.11 shows LEVEL 3 of software for computing the saturation measurements (Goodman and Corenman 1990). The system starts by acquiring a potential optical pulse after a DATA FLAG has been set and inquiring whether there is ECG synchronization i.e., a regular ECG period has been established. If a DATA FLAG has not been set, then the system exits the routine. If there has not been ECG synchronization, then the microprocessor processes the optical pulse signals independent of the ECG.

MASIMO 2053
Apple v. Masimo
IPR2022-01300
APL_MAS_ITC_00015781
RX-0035.0164

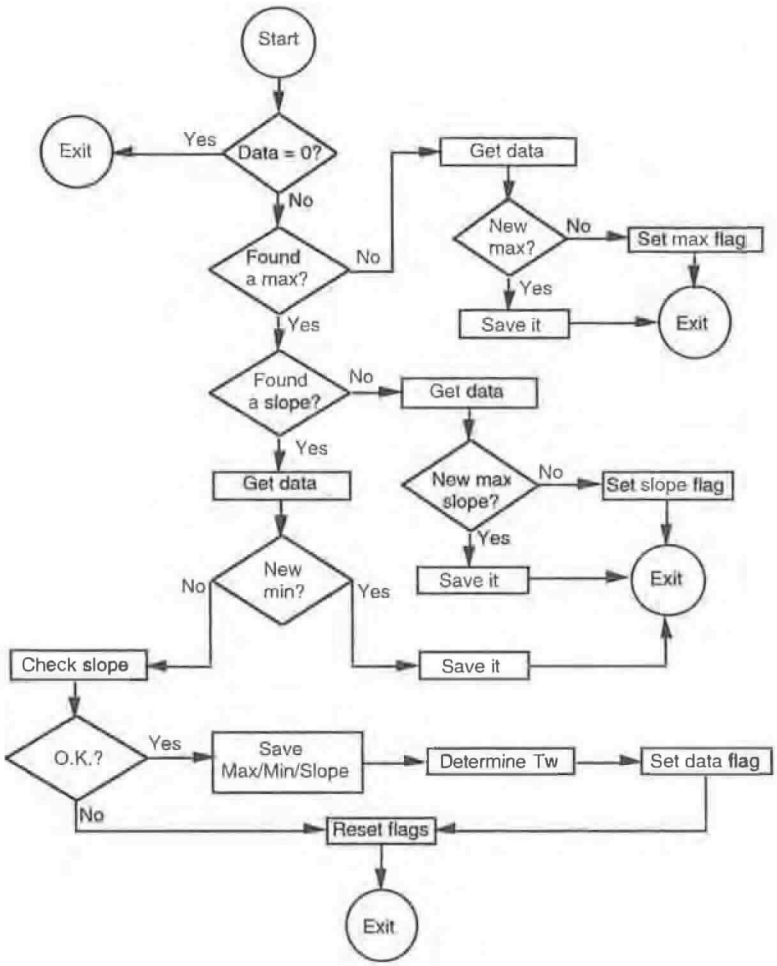

Figure 9.10. The system routine measures the maximum and minimum values in the data presented and calculates the largest slope. The slope value is compared with the normal expected values to determine whether it is a possible optical pulse (Goodman and Corenman 1990).

If there is ECG synchronization, but no R wave has occurred, then the system exits and the pulse is not processed. If there is ECG synchronization and a R wave has occurred, then the microprocessor processes the pulse. The LED intensity is evaluated to see if adjustment is necessary. The reset system gain, based on minimum LED intensity required for adequate signal strength, is checked to see if adjustment is required to the optical pulse historic period, amplitude and ratio. The system then inquires whether the ECG apparatus is operating between an R wave and the following optical pulses for the previous four pulses is computed to give the TIME WINDOW (TW). Then the pulse waveform is analyzed to see if it is a dicrotic notch rather than a real optical pulse. The downward slope of a dicrotic notch or other artifact can be

MASIMO 2053
Apple v. Masimo
IPR2022-01300
APL_MAS_ITC_00015782
RX-0035.0165

misinterpreted as an optical pulse, but typically the pulse amplitude is less than half the amplitude of an actual pulse. If the pulse is determined to be a notch or artifact, then the system exits and the next pulse presented will be processed. If not determined to be a notch, then it is analyzed to determine if it is a pulse.

Assuming the ECG is synchronized, then the system determines if two criteria are met. The first is whether the time delay falls within the above-computed TIME WINDOW. If it does not, then the microprocessor rejects the pulse. The second criterion tested is whether or not the ratio is within acceptable limits. Only if the pulse satisfies both criteria is the pulse accepted and a saturation calculation made.

If the ECG is not synchronized then the pulse must pass any two of three criteria regarding (1) pulse period, (2) amplitude, and (3) ratio, to be accepted, e.g., pulse and period, period and amplitude, pulse and amplitude, or all three. If the pulse is accepted, then the oxygenation saturation is calculated.

After the system is turned on (POWER UP) after a TIME OUT alarm (a 10 s period with no valid optical pulse found) a series of consistent pulses must be found to generate an optical pulse history before the oxygenation saturation will be sent to the display. Thus, if there is no optical pulse synchronization, there will be no saturation display. All optical pulses, those accepted and those not accepted, excluding pulses rejected as artifacts, enter the calculation routine section. If the ECG is not synchronized then a pulse-to-pulse period and either an amplitude or a ratio must exist for the optical heart rate (OHR) calculation to be made. If either the ECG or the optical pulse is synchronized, then the HR calculation made will be displayed. If there is no synchronization, then the OHR is not displayed. The system is evaluating the status for pulse evaluation, i.e., whether signals should continue to be processed after a TIME WINDOW period has expired then TIME WINDOW is closed until opened by the detection of the next R wave. The blood oxygen saturation is calculated using the Ratio of Ratios.

9.6.2 Criticare® systems

The patient wears three standard ECG electrodes which provide the pulse oximeter with an ECG signal which if present is used to enhance the quality of the optical waveforms. The oximeter computes oxygen saturation from the enhanced waveform and displays it on a screen (Conlon *et al* 1990).

An ECG amplifier and an R-wave detection algorithm routine process the ECG signal provided by the electrodes and determine the timing for an ensemble averaging algorithm routine. An oxygen saturation value is calculated by a microcomputer in a calculation algorithm routine using the ensemble averaged waveform as input, and is then displayed digitally on a screen.

If an ECG signal is not present, the absence is detected by the R wave detection algorithm routine which causes the ensemble averaging routine to be bypassed and the unenhanced optical pulse to be input into the calculation algorithm routine. The microcomputer executes the software comprising the R wave detection, ensemble averaging, calculation, and display algorithm routines.

The three lead ECG signal is amplified by a differential amplifier. This amplifier amplifies the differential component of the signal, which is the desired ECG waveform, while rejecting a large portion of the common-mode voltage. The output of this amplifier is AC-coupled by a capacitor to an amplifier which provides further gain. The gain provided by the amplifier is adjustable and can be set to 1/2 or 2 by the microprocessor. The amplifier can also accept an additional

MASIMO 2053
Apple v. Masimo APL_MAS_ITC_00015783
IPR2022-01300
RX-0035.0166

high level input which is intended to be connected to the output of an external ECG monitoring device, thus obviating the need for an additional set of ECG electrodes on the patient. The output of the amplifier is processed by a low-pass filter to remove the unwanted artifact such as 60 Hz and electrosurgery induced noise, and is converted to a serial, digital signal by an ADC. The digitized signal then passes through an optoisolator to a serial port which resides on the bus of the microcomputer. The optoisolator serves to isolate the patient ECG leads from the external power supply and is incorporated for reasons of patient safety.

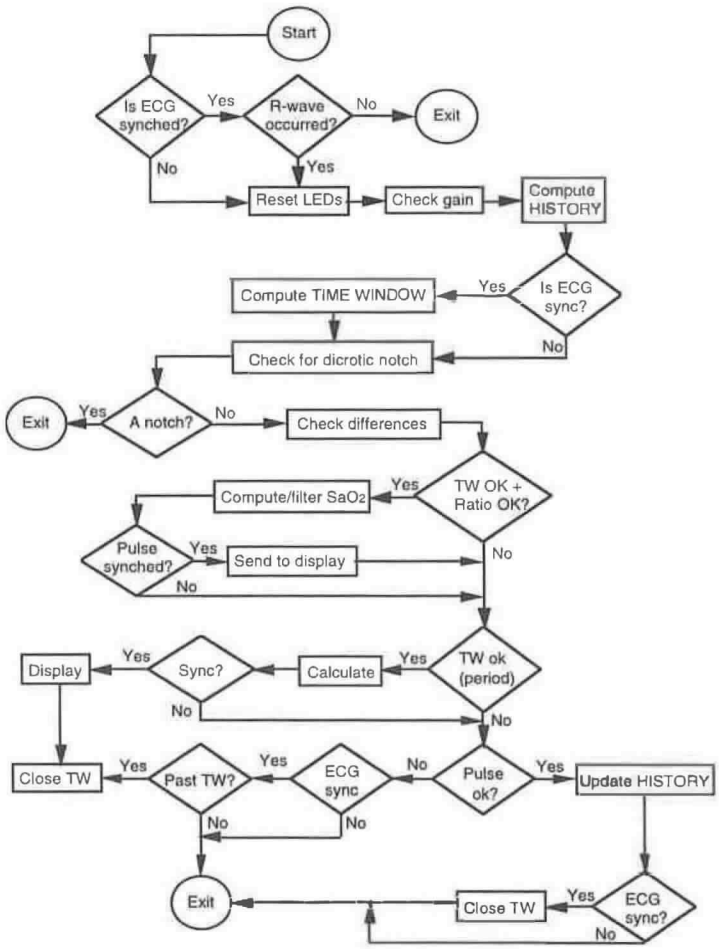

Figure 9.11. The LEVEL 3 software checks for ECG synchronization and processes the data appropriately to calculate the oxygen saturation (Goodman and Corenman 1990).

The oximeter is software driven and the operation of the software involves the process of removing motion artifact and enhancing waveform quality in low perfusion situations.

MASIMO 2053
Apple v. Masimo
IPR2022-01300
APL_MAS_ITC_00015784
RX-0035.0167

ECG synchronization is used to provide a reliable time frame upon which to base ensemble averaging, and a robust and accurate R wave detection algorithm is an integral part of the system. The R wave detection process involves three stages of processing: a low-pass digital filter, a peak excursion finding algorithm and a peak discrimination algorithm. The ECG input signal from the ADC is sampled at a rate of 240 Hz. The resulting digital waveform is low-pass filtered, with a corner frequency of 12 Hz, to remove artifact such as 60 Hz and muscle noise.

9.6.2.1 Peak excursion finding algorithm. The filtered ECG waveform then undergoes transformation by the *peak excursion finding algorithm*. The purpose of this transformation is to amplify those characteristics of the ECG waveform which are inherent in QRS complexes while inhibiting those which are not (Conlon *et al* 1990). This algorithm continually matches the ECG waveform to one of the two templates as shown in figure 9.12. The algorithm maintains a queue buffer of length N, which is searched in order to determine the parameters P1, P2, P3, and P4. The algorithm routine is called for $N = 8$, 12, 16, 20, and 24, and the individual excursion values are summed so as to give a total transformation value. More weight is placed on lower values of N in order to emphasize narrower spikes over wider ones. The newest sample is added to the buffer at each instant and the oldest sample is removed from the buffer. The maximum and the minimum values and their positions are searched in the buffer and depending on their relative positions, the matched template is chosen. The parameters P2 and P3 are assigned the appropriate maximum and minimum values accordingly. The parameters P1 and P4 are then found based on the template. For example, if the buffer matches template (a), the maximum value after P2 is assigned to P1, and the minimum before P3 is assigned to P4. Finally, the peak closed excursion on the interval N is computed as (P3 – P2 – (P4 – P1)) if the buffer matches template (a) or (P2 – P3 – (P1 – P4)) if the buffer matches template (b).

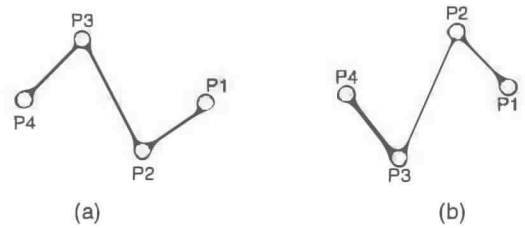

Figure 9.12. Two ECG waveform templates utilized in R-wave detection.

9.6.2.2 Peak discrimination algorithm. After transformation of the ECG waveform, the peak discrimination algorithm classifies the spikes found in the transformed waveform as either QRS complexes or artifact. The peak discrimination algorithm is a state machine with three states: peak, valley, and noise peak. The thresholds are set based upon the past history of the ECG waveform.

The algorithm enters the peak state if the algorithm is in the valley or noise state and exceeds a set threshold (threshold 2). The algorithm exits the peak state and enters the valley state when the waveform drops below one fourth of the maximum value attained in the peak state. The algorithm in valley state enters the

MASIMO 2053
Apple v. Masimo
IPR2022-01300
APL_MAS_ITC_00015785
RX-0035.0168

noise state whenever the waveform climbs above four times the minimum value attained during the valley state. The algorithm in noise state enters the valley state when the waveform drops half the distance between the maximum value attained during the noise state and the minimum during the previous valley state. The detection of QRS spike is signaled upon the transition into the peak state. The conditions for state changes are summarized in the table 9.1. The algorithm maintains an average of the last eight QRS peaks in order to set the threshold for detecting the next peak in the waveform. An average of the noise peak levels found between the last four QRS peaks, is also maintained to aid the rejection of artifact while accepting valid QRS spikes. The averages are updated whenever there is a transition between the peak and valley states.

Table 9.1 A summary of conditions for state changes.

Present state	Condition	Next state
Valley or Noise states	Exceeds a set threshold	Peak state
Peak state	< 1/4 max in peak state	Valley state
Valley state	> 4* min in valley state	Noise state
Noise state	< 1/2 (max in noise – min in previous valley)	Valley state

Additional rejection of artifact is gained by examining the length of time which has elapsed between a new peak and the last accepted peak (interval figure 9.15). If it is less than 5/8 of the previous R–R interval, the spike is assumed to be noise and is not counted as a QRS spike. If it is greater than 7/8 of the previous R–R interval, it is accepted unconditionally. If it is greater than 5/8, but less than 7/8 of the previous R–R interval, the spike is accepted on probation as long as it exceeds a second threshold (threshold 1) which is set based on the noise peaks encountered during the last four beats. It is counted as a valid QRS spike but the previous state information is also saved in order to undo acceptance of the spike if a better candidate is found. The probation interval is equal to 9/8 of the previous R–R interval minus the length of time which has elapsed since the last accepted peak. During this interval any spike which meets the threshold requirements overrides the acceptance of the spike in question.

When the algorithm is found to be in the peak state, the maximum value encountered in this state is noted. If the waveform is not a local maximum, the routine checks to see if the waveform has fallen to one fourth of the last local maximum. If it has, the routine determines whether the current peak is a noise peak or a QRS peak. If it was a noise peak, the average of the noise levels over the last four beats is calculated. If it was a QRS peak, the average of the last eight QRS peaks is updated using the local maximum. The threshold values needed to detect the next QRS peak are then determined. Threshold 1 is halfway between the current eight-beat peak average and the current four-beat noise average. Threshold 2 is one-half of the current eight beat peak average (figure 9.13).

Before exiting the peak discrimination algorithm, parameters reflecting the quality of the ECG waveform are tested. If the time elapsed since the spike was accepted exceeds four times the R–R interval and/or the baseline of the transformed signal exceeds one-half the peak value, the ECG waveform is assumed to be lost and the routine disengages the synchronization.

9.6.2.3 Ensemble averaging algorithm. The ensemble averaging algorithm makes use of the output of the R–wave peak discrimination algorithm to enhance that

MASIMO 2053
Apple v. Masimo
IPR2022-01300
APL_MAS_ITC_00015786
RX-0035.0169

part of the red and infrared plethysmographic waveforms which are correlated with the ECG, while diminishing all which is unrelated, to yield a signal with an improved signal to noise ratio (Conlon *et al* 1990).

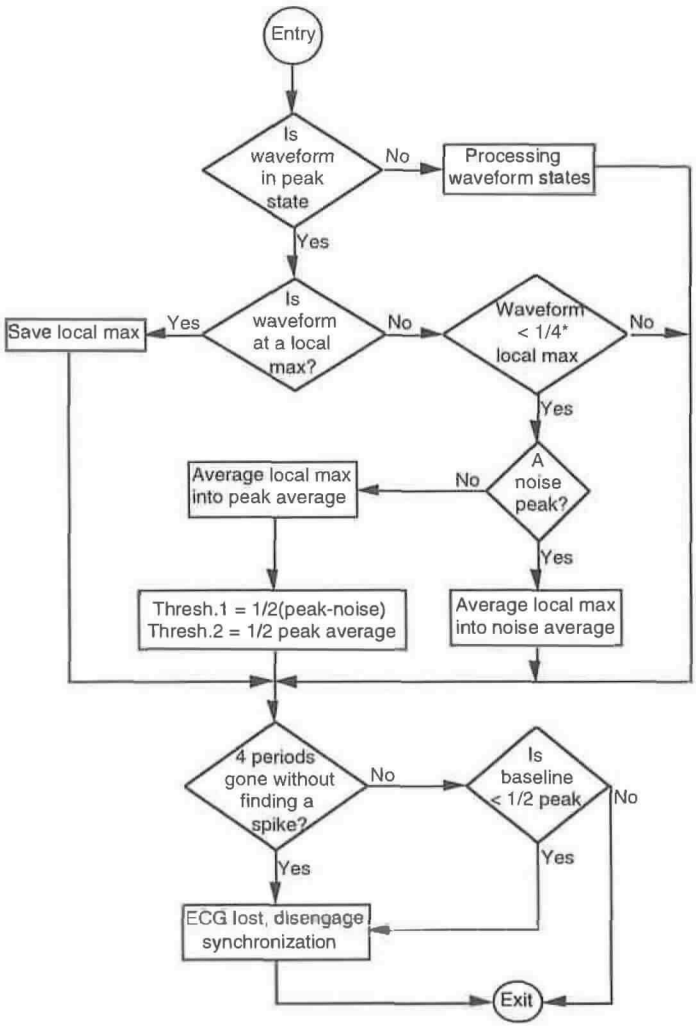

Figure 9.13. The R wave peak discrimination algorithm (Conlon *et al* 1990).

The algorithm relies on the assumption that instances of moderate to severe motion, and of low perfusion, can be detected as the plethysmographic waveforms are being sampled (figure 9.14). To do this, it was found to be advantageous to buffer these waveforms while they are being sampled, and to delay the actual averaging until the R peak is detected. The averaging weight of the current waveform cycle can then be adjusted, depending on whether the plethysmographic waveform just acquired is weak or exhibits the influence of

MASIMO 2053
Apple v. Masimo
IPR2022-01300
APL_MAS_ITC_00015787
RX-0035.0170

excessive motion artifact. An additional benefit of this buffering stage is that the oximeter is able to discard waveform pulses during which optical pulse processing circuitry has saturated and distorted the waveform. Yet another benefit of this buffering stage is that it allows a level of error tolerance in the R wave detection process whereby the peak_discrimination routine can accept certain marginal QRS spikes on probation while maintaining the flexibility to correct the error if a better candidate is subsequently detected (figure 9.15).

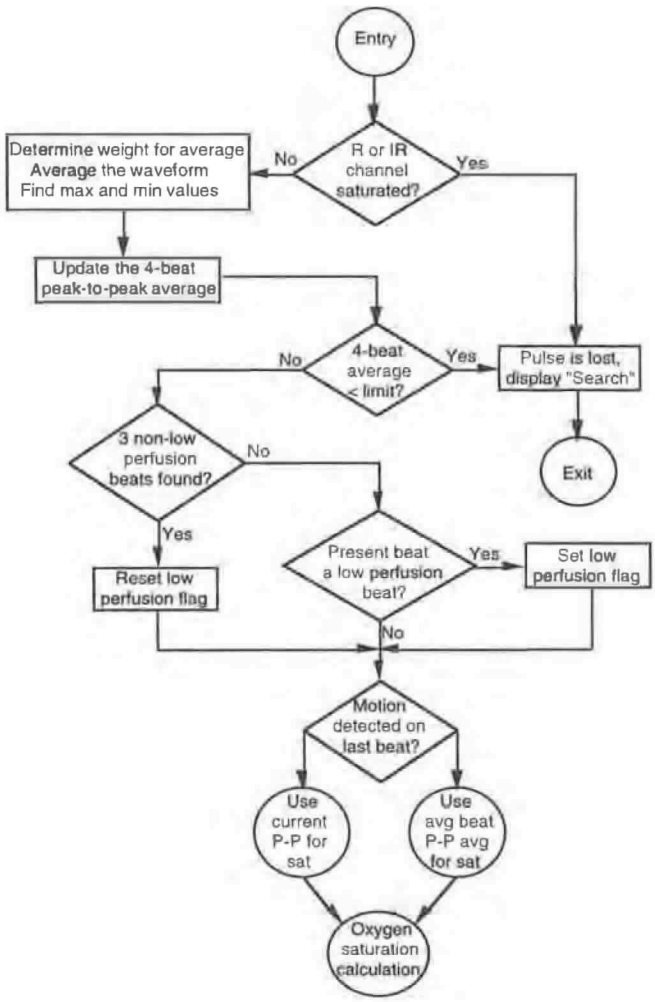

Figure 9.14. The ensemble averaging algorithm (Conlon *et al* 1990).

9.6.2.4 Motion determination algorithm. In order to give less weight to waveform pulses which are distorted by motion artifact, a criterion by which motion can be measured is established. This routine assumes that a plethysmograph unaffected by motion varies only slightly between one pulse and

MASIMO 2053
Apple v. Masimo
IPR2022-01300
APL_MAS_ITC_00015788
RX-0035.0171

the next. In addition, a change in the amplitude, not shape, of the pulse comprises the majority of the observed difference between one pulse and the next. A plethysmograph containing artifact, however, differs greatly from the previous signal. A point-by-point subtraction of the latest pulse from the one preceding it yields a signal with an average amplitude less than that of the signal. The value of the difference signal is more or less constant while the signal itself changes rapidly. The integration of the difference signal yields a good indication of the amount of motion present in the pulse. A noisy signal yields a large value on integration compared to a clean signal. This routine checks for the occurrence of an R-wave spike which would be detected by the R-wave detection algorithm. If a spike was detected, the routine saves the integrated value as an indication of the level of motion present in the pulse, and initializes the variables to prepare for the next pulse (Conlon *et al* 1990).

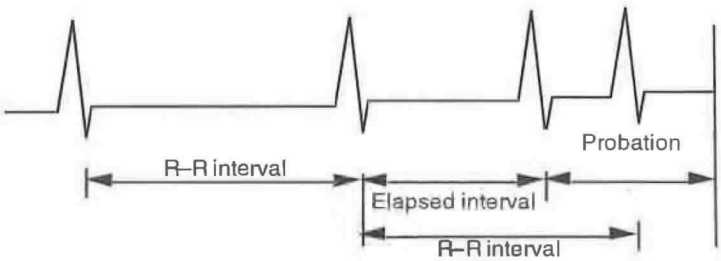

Figure 9.15. R wave artifact rejection timing subroutine (Conlon *et al* 1990).

9.6.2.5 Pulsatile waveform weight determination algorithm. It is generally known that ensemble averaging with a set of N waveforms increases signal-to-noise ratio by a factor of the $\sqrt{N}$ for uncorrelated, random noise. Thus, ensemble averaging will decrease the influence of the uncorrelated motion artifact and will enhance a low perfusion signal (which may be buried in noise) at the expense of response time. At the same time, a maximum limit on response time is set in order to ensure that the displayed saturation value is reasonably current (Conlon et al 1990).

The variable weight average is used in order to provide flexibility over a broad spectrum of pulsatile waveforms. It attempts to give a large weight to waves which are largely motion-free, while diminishing the weight given to those which have motion. Additionally, if a low perfusion situation is detected, less weight is given to all pulses until several strong pulses are found. Furthermore, the algorithm takes into account the pulse rate when determining the averaging weight. Since the averaging occurs each time a beat is detected, more averaging can be used on a patient with a fast pulse rate than one with a slow pulse rate while maintaining a constant response time. More averaging is needed in cases of motion artifact and low perfusion because the signal-to-noise ratio of these pulses is less than normal pulses (figure 9.16).

The weight determination algorithm uses two empirically determined thresholds to determine whether the motion is significant. One of these thresholds applies during the normal perfusion, while the other is used in cases of low perfusion. The algorithm decides which of the two thresholds to use by checking for the low perfusion state. If the low perfusion has not been detected, the

MASIMO 2053
Apple v. Masimo
IPR2022-01300
APL_MAS_ITC_00015789
RX-0035.0172

algorithm checks the motion against the high motion threshold. If significant motion is not found, the algorithm checks whether the heart rate is above 120 bpm. If it is, the beat is assigned an average weight of 1/8, otherwise an average weight of 1/4. If significant motion is found, the algorithm checks for the heart rate and if it is above 120 bpm, assigns an average weight of 1/16. Further, if the heart rate is below 60 bpm, the algorithm assigns an average weight of 1/8.

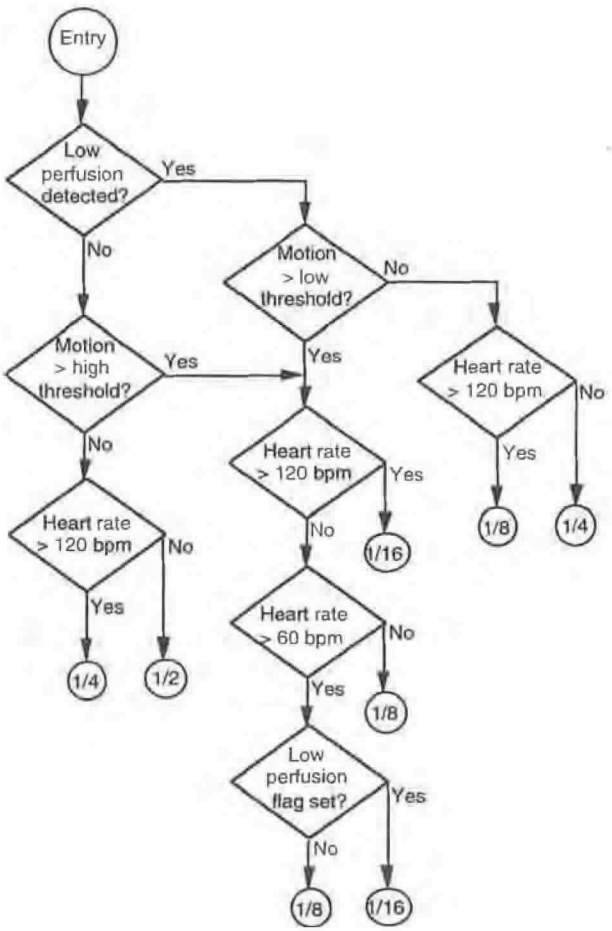

Figure 9.16. The weight determination algorithm (Conlon *et al* 1990).

If the heart rate is above 60 bpm and less than 120 bpm, the software has to differentiate between low perfusion with motion and motion alone. The algorithm checks the low perfusion flag and if set, assigns an average weight of 1/16, otherwise it assigns a weight of 1/8. The ensemble_averaging routine employs the

MASIMO 2053
Apple v. Masimo
IPR2022-01300
APL_MAS_ITC_00015790
RX-0035.0173

weight determination algorithm to find the average weight of the waveform and averages the buffered waveform with the composite averaged waveform stored in the microcomputer memory using a tail-weight average of the form (W × NEW) + (1 − W) × COMPOSITE, with W being the averaging weight. Because the averaged pulses are of varying duration, some pulses will overlay more points of the averaged waveform than others. Thus, the tail of the averaged waveform may not accurately reflect the most recent plethysmographic information. Hence the minimum and maximum of the averaged waveform were found only up to the minimum length of the last eight pulses. After determining the minimum and maximum values, the four beat average of peak-to-peak values are updated.

The algorithm then checks to ensure that the average has not fallen below the minimum low perfusion threshold. If it has, the pulse is considered lost. Then the algorithm checks if three non-low perfusion beats have been found. If so, it resets the low perfusion flag. If not, it checks if the current beat is a low perfusion beat, setting the perfusion flag appropriately. The algorithm then checks for motion in the last beat. If there is motion, it sends the four-beat, peak-to-peak average to the saturation_calculation algorithm routine. Otherwise, the last peak-to-peak value of the routine is sent to the saturation_calculation algorithm which calculates the oxygen saturation and displays it.

9.7 SPECTRAL METHODS OF ESTIMATING S_pO_2

Arterial oxyhemoglobin saturation (S_pO_2) values are currently computed using weighted moving average (WMA) techniques (Rusch *et al* 1994). These methods process the time domain signals and give a precision of no better than ± 2% (± one standard deviation). Researchers have explored other digital signal processing algorithms for improved estimation of S_pO_2. The fast Fourier transform (FFT) and discrete cosine transform (DCT) were identified as potentially superior algorithms (Rusch *et al* 1994) and useful to optimize the portability of pulse oximetry systems. Preliminary studies indicate that a 64-point FFT, with a 15 Hz sample rate, over a data collection period of 4.3 s was found to be the optimal combination for pulse oximetry applications, minimizing hardware expense, footprint, and power consumption. S_pO_2 values were calculated from a transform size of 64 points using

$$S_pO_2 = 110 - 25 \times R \tag{9.36}$$

where R is the ratio of the red and infrared normalized transmitted light intensity. The R value is

$$R = \frac{AC_R/DC_R}{AC_{IR}/DC_{IR}}. \tag{9.37}$$

The AC component is the signal variation at the cardiac frequency and the DC component is the average overall transmitted light intensity. The AC component is selected as the highest spectral line in the cardiac frequency band.

MASIMO 2053
Apple v. Masimo
IPR2022-01300
APL_MAS_ITC_00015791
RX-0035.0174

REFERENCES

Cheung P W, Gauglitz K, Mason L R, Prosser S J, Smith R E, Wagner D O and Hunsaker S W 1989 Feedback-controlled method and apparatus for processing signals used in oximetry *US patent 4,819,646*

Cheung P W, Gauglitz K, Mason L R, Prosser S J, Smith R E, Wagner D O and Hunsaker S W 1990 Method and apparatus for offsetting baseline portion of oximeter signal *US patent 4,892,101*

Conlon B, Devine J A and Dittmar J A 1990 ECG synchronized pulse oximeter *US patent 4,960,126*

Corenman J E, Stone R T, Boross A, Briggs D A and Goodman D E 1990 Method and apparatus for detecting optical signals *US patent 4,934,372*

Frick G, McCarthy R and Pawlowski M 1989 Waveform filter pulse detector and method for modulated signal *US patent 4,867,571*

Goodman D E and Corenman J E 1990 Method and apparatus for detecting optical signals *US patent 4,928,692*

Jaeb J P and Branstetter R L 1992 Composite signal implementation for acquiring oximetry signals *US patent 5,094,239*

Pologe J A 1987 Pulse oximetry: technical aspects of machine-design *Int. Anesthesiol. Clinics* **25** 137–53

Potratz R S 1994 Condensed oximeter system with noise reduction software *US patent 5,351,685*

Scharf J E and Rusch T L 1993 Optimization of portable pulse oximetry through fourier analysis *Proc. IEEE Twelfth Southern Biomedical Engineering Conf.* Tulane University pp 233–5

Smith R E 1989 Method and apparatus for processing signals used in oximetry *US patent 4,800,495*

Stone R T and Briggs D A 1992 Method and apparatus for calculating arterial oxygen saturation based plethysmographs including transients *US patent 5,078,136*

Yorkey T J 1996 Two 'rat rat' derivation *Personal communication* (Hayward, CA: Nellcor Inc)

INSTRUCTIONAL OBJECTIVES

9.1. Name the general sources of error that could be corrected with signal processing algorithms.
9.2. Explain the process of eliminating incident light intensity and thickness of the path as variables from Beer–Lambert law.
9.3. How is R_{OS} (Ratio of Ratios) estimated from the red and infrared optical signals?
9.4. Discuss the advantages of estimating R_{OS} using the derivative method over the peak and valley method. Explain how noise reduction is achieved using the derivative method.
9.5. Discuss the role of the construction–reconstruction process in improving the accuracy of S_aO_2 estimation.
9.6. Explain the function of the start-up interrupts.
9.7. Discuss the function of the five different states in the period zero subroutine.
9.8. Discuss the C-Lock ECG synchronization algorithm used in Nellcor[®].
9.9. Explain the motion detection algorithm used in Criticare.
9.10. Name the advantages of using spectral methods in estimating oxygen saturation.
9.11. Explain the advantages of using ECG synchronization.

MASIMO 2053
Apple v. Masimo
IPR2022-01300
APL_MAS_ITC_00015792
RX-0035.0175

CHAPTER 10

CALIBRATION

Jeffrey S Schowalter

The calibration curves of *R* (Ratio of Ratios) values used to calculate oxygen saturation levels are critical to the accuracy of the entire pulse oximeter system. Without an accurate table of appropriate *R* values, the pulse oximeter has no way of determining oxygen saturation levels. As such, it is important to understand how the pulse oximeter calibration curve data are acquired. In addition, it is important to understand some of the past and present simulation techniques used to test the accuracy and functionality of pulse oximeters.

10.1 CALIBRATION METHODS

Chapter 4 states that Beer's law does not apply for a pulse oximetry system due to the scattering effects of blood. Therefore, pulse oximeter manufacturers are currently forced to use an empirical method of determining the percentage of arterial oxygen saturation for a given *R* ratio.

10.1.1 Traditional in vivo calibration

The traditional method of pulse oximeter calibration involves comparison of oximeter *R* value to the oxygen saturation ratio obtained from *in vivo* samples using human test subjects. In fact, this was the only method used to calibrate these devices up until 1993 (Moyle 1994). Although this method requires a variety of laboratory instrumentation and is typically done in a hospital setting, this data collection process is only required during the design and development of the device.

10.1.1.1 Procedure. In general, the calibration procedure is fairly straightforward. Test subjects are fitted with an indwelling arterial cannula, which is placed in the radial artery. A sample of blood is taken and analyzed with a CO-oximeter (see chapter 3) to determine the subject's levels of COHb and MetHb. In most cases, samples are taken over a broad population. Typically, data come from nonsmokers with background carboxyhemoglobin levels between 1% and 2%. Wukitsch *et al* (1988) mentions that subjects used for the Ohmeda Biox 3700 calibration had an average COHb level of 1.6% and a MetHb level of 0.4%.

MASIMO 2053
Apple v. Masimo
IPR2022-01300
APL_MAS_ITC_00015793
RX-0035.0176

Once a low level of COHb and MetHb are verified, the subject is also fitted with one or more pulse oximeter probes. The test begins by first ensuring that the subject is at the 100% oxygen saturation level. The subject breathes an oxygen/air mix so as to bring the arterial oxygen saturation level to 100% (as determined from arterial blood analyzed with the CO-oximeter). Oxygen saturation level is incrementally decreased by breathing gas mixtures of progressively less oxygen and more nitrogen. At each level where the pulse oximeter indicates a stable reading, an arterial blood sample is immediately taken and analyzed with the CO-oximeter. Corresponding readings are recorded and the data are then plotted with oxygen saturation percentage (as determined by the CO-oximeter) on the y-axis and R ratio (as determined by the pulse oximeter under test) on the x-axis yielding a traditional R curve as shown in figure 4.7. Typical values for the R ratio vary from 0.4 to 3.4 (Pologe 1989). A best fit calibration equation is then calculated from the data. If the pulse oximeter manufacturer has selected LEDs for their probes that have relatively narrow bands of center wavelength (as discussed in chapter 5), then only one curve is required. If they have a number of probes with differing red and infrared center wavelengths, then each probe with unique LED combination must be tested to obtain its unique curve characteristics. Some manufacturers have as many as 30 different probes.

10.1.1.2 Problems. One of the problems with this traditional method is the limited range of oxygen saturation that can be acquired. Ethical issues prevent intentional desaturation of healthy subjects below a certain point due to risk of hypoxic brain damage. As a result, saturation levels can only be reduced to around 60%. This leaves a large range of values on the curve that need to be calculated by extrapolation. This has the potential to induce errors and in fact, Severinghaus *et al* (1989) tested 14 pulse oximeter models and showed that most pulse oximeters performed poorly under relatively low levels of saturation (see chapter 11). Another problem of this calibration method is that it does not address the spacing and number of data points needed to build a curve. Moyle (1994) states that well spaced data points over the entire range from 100% down to 80% is more accurate than having many data points clustered between 95% and 100%.

There has been a great deal of debate over the years as to what the pulse oximeter is actually measuring and as such, a unique term has been created to specify an oxygen saturation reading as determined by a pulse oximeter. The problem is that the pulse oximeter uses two wavelengths to measure oxygen saturation. However, there are four common species of hemoglobin (Hb, HbO_2, COHb, and MetHb). Since there are routinely four light absorbing substances in a sample in a system which is assuming it is measuring only two substances, much discussion and misconception arise as to what the pulse oximeter is actually measuring (Pologe 1989). Equation (4.5) shows that functional S_aO_2 is the ratio of oxygenated hemoglobin to the sum of oxygenated and reduced hemoglobin. If a person were found that had no COHb or MetHb, this is what the pulse oximeter would measure. However, since some COHb and MetHb are typically present in everyone's blood, and these terms show up in the fractional S_aO_2 formula, it is easy to assume that the pulse oximeter is measuring fractional S_aO_2. However, this is not the case either. Moyle (1994) state that the conventional two-wavelength oximeter measures what should be defined as 'oxygen saturation as measured by a pulse oximeter', or S_pO_2.

MASIMO 2053
Apple v. Masimo
IPR2022-01300
APL_MAS_ITC_00015794
RX-0035.0177

Payne and Severinghaus (1986, p 47) state that the pulse oximeter reports

$$\frac{HbO_2 + COHb + MetHb}{HbO_2 + COHb + MetHb + Hb} \times 100\% \qquad (10.1)$$

and subtracting this quantity from 100% gives the percentage of reduced hemoglobin or Hb%. He suggests that to eliminate confusion pulse oximeters should display this value instead. If this were done, however, conventional thinking would have to change because readings would increase from zero as opposed to S_pO_2 readings which decrease currently from 100. The bottom line is that COHb and MetHb do have an effect on the accuracy of pulse oximeter readings (Reynolds *et al* 1993a,b) so they cannot be ignored as part of the calibration process.

10.1.1.3 Effects of COHb and MetHb. The effects of COHb and MetHb are typically handled in one of two ways. Some manufacturers subtract 2% for these factors so they are displaying fractional saturation (assuming a patient with nominal levels of COHb and MetHb) and others do not subtract this factor so they are displaying functional saturation (Ackerman and Weith 1995).

In a sense, the pulse oximeter will measure what it has been calibrated to measure based on the test subject profile. Tremper (Payne and Severinghaus 1986) states that Nellcor calibration data were originally based on five Olympic athletes in virtually perfect physical condition. These individuals probably had as low levels of COHb and MetHb as are found in humans. As such, anyone being tested with higher (normal) levels of COHb and MetHb yielded inaccurate readings. Today, by using a more representative subject to build the calibration curve, pulse oximeter manufacturers account for some of this during the calibration process. However, individuals with relatively high levels of COHb and MetHb will have inaccurate S_pO_2 readings.

10.1.1.4 Field calibration. Another issue of concern is field calibration. Using this technique, once the *R* curves are established, the transmitting wavelengths of the LEDs and corresponding *R* curve are provided via a coding resistor (see chapter 5) and as such only a two-point check to verify the correctly selected calibration curve is required. Typically this check will identify a problem due to a malfunctioning LED or photodiode or an incorrect coding resistor. However, other than this cursory check there is no type of field calibration done on the pulse oximeter. Cheung *et al* (1993) have proposed a system for compensating for the effects of temperature variations on the LEDs. Since the pulse oximeter photodiode cannot detect a shift in LED wavelength, the proposed system provides the capability for the temperature of the probe LEDs to be measured and thus an alternative calibration curve, as shown in figure 10.1, can be used for the new set of LED wavelengths. This system seems to be of limited usefulness however, since Reynolds *et al* (1991) have shown that the peak wavelength of a red LED will only shift by 5.5 nm and an infrared LED will shift by 7.8 nm with a temperature shift from 0 °C to 50 °C. Applying this information to a theoretical computer model based on Beer's law, causes negligible changes in accuracy of the pulse oximeter.

MASIMO 2053
Apple v. Masimo
IPR2022-01300
APL_MAS_ITC_00015795
RX-0035.0178

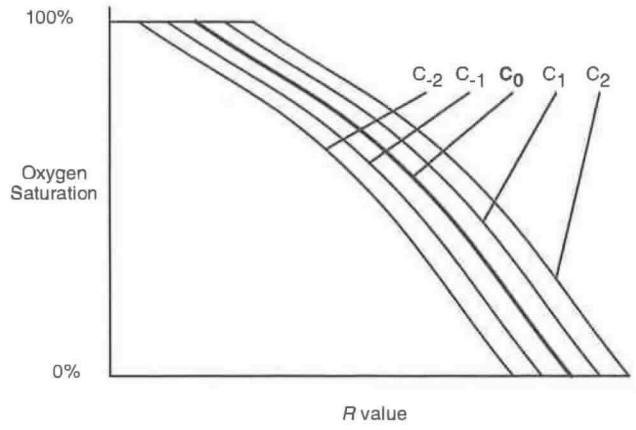

Figure 10.1 Temperature compensation curves as proposed by Cheung *et al* (1993). C values indicate different curves for use with different sensed temperatures.

10.1.2 In vitro calibration using blood

Figure 10.2 shows an *in vitro* test system that requires whole blood (Reynolds *et al* 1992). Blood is pumped through a cuvette acting as a model finger. The pulse oximeter probe is then attached to the model finger. Blood is pulsed within the system using a computer controlled peristaltic pump head capable of generating almost any shape of pulsatile waveform. Blood is oxygenated by passing through a membrane oxygenator using a gas mixture of O_2, N_2, and CO_2. The composition of the gas mixture passing through the membrane oxygenator is controlled with a gas mixing pump. A variety of model fingers were tried with the final model finger consisting of a cuvette made of two thin (0.5 mm) silicone rubber membranes and a rigid Plexiglas central section. When using whole blood, the model finger is covered with a diffuser made from translucent paper. Blood enters one end of the cuvette and flows in a thin (1 mm) layer through the cuvette over the fingertip end and back along the bottom side. Both inlet and outlet are tapered to prevent flow separation. The silicone rubber membrane is flexible enough such that pulsating blood produced volume changes in the tubes giving an AC/DC ratio in the physiological range. Readings from the pulse oximeter are recorded and a simultaneous sample taken from the sample port and analyzed by the CO-oximeter in a similar fashion to the procedure described in section 10.1.1. This system yields calibration values that are accurate to 50% and lower. Most pulse oximeters have no specified accuracy below 50%. One problem is that the system is sensitive to blood flow rate, due to changes in blood cell orientation with flow. This was verified using a hemoglobin solution instead of whole blood in the test system.

MASIMO 2053
Apple v. Masimo
IPR2022-01300
APL_MAS_ITC_00015796
RX-0035.0179

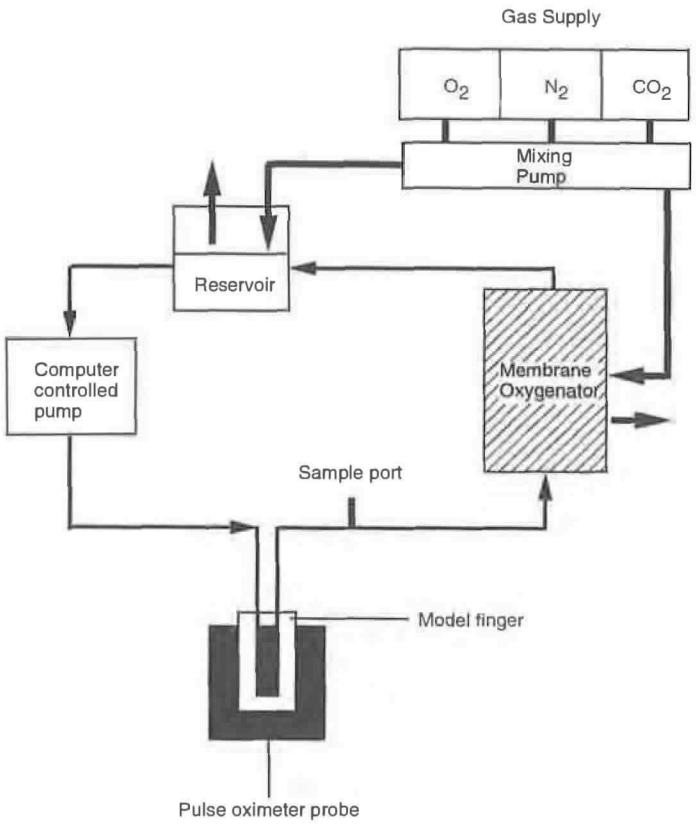

Figure 10.2 Block diagram of *in vitro* test system developed by Reynolds *et al* (1992).

10.2 TESTING SIMULATORS

Devices which check the functionality of pulse oximeters are becoming increasingly popular. Many of these devices use some type of artificial finger to verify that the pulse oximeter is functioning correctly. When pulse oximeters first came out, the only way technicians had to verify the functionality of the pulse oximeter was to use their own fingers. This, however, only indicates basic functionality at best with no way to control any parameters and with nothing with which to compare. Several devices have been developed that simulate the optical properties of the human finger and its pulsatile blood flow. In addition, optoelectronic systems, which simulate the human finger electronically, have also been developed. Finally, pulse oximeter manufacturers themselves have developed simple simulators that essentially simulate a probe's electron signals.

MASIMO 2053
Apple v. Masimo
IPR2022-01300
APL_MAS_ITC_00015797
RX-0035.0180

10.2.1 Simulators using blood

Several simulators have been proposed that need whole blood to test the functionality of the pulse oximeter. These simulators are all based on the concept of being able to simulate the absorbance of human tissue (normally the finger) between the LEDs and the photodiode of the pulse oximeter under test. Since few substances have been found that simulate the optical properties of blood, these types of systems typically provide the most accurate simulation.

10.2.1.1 Reynolds system. The system described in section 10.1.2 functions equally well as a simulator to test the functionality of pulse oximeters. In fact this system has been used to compare ten commercially available oximeters (Reynolds *et al* 1992), and has been used to evaluate the effects of dyshemoglobins on pulse oximeter accuracy (Reynolds *et al* 1993a,b). However, this *in vitro* test system is not practical in a hospital setting where most pulse oximeters are used. The system requires a laboratory setting, is not portable, uses oxygenated whole blood and needs a CO-oximeter for comparison. However, this instrument is generally considered the *gold standard* for calibrating and testing a pulse oximeter over its complete range.

10.2.1.2 Vegfors system. The Vegfors system is similar to the Reynolds system but with a focus on the artificial finger or 'finger phantom' used. Vegfors *et al* (1993) describe a system where their artificial fingers consist of silicone rubber tubes inserted in plastic Delrin cubes. The tubing system chosen was based on its characteristics of tubing diameter, wall elasticity, and blood flow velocity to simulate normal physiological characteristics of blood in motion. Delrin was used because it has similar optical scattering properties to human tissue. Figure 10.3 shows three models. Two different finger models, one with one tube and another with five tubes were tested along with a third artificial finger consisting of 15 silicone rubber tubes mounted in silicone rubber in the form of glue. The object was to develop an optical model which simulated the arterial bed of the human finger containing blood vessels and surrounding tissue. The results of these different finger configurations determined that physical dimensions of the artificial bed are of minor significance for pulse oximeter readings.

10.2.1.3 Single wedge system. Several other less complicated simulators using whole blood have been proposed. In one system, proposed by Yount (1989), a light-absorbing wedge shaped vessel containing blood of known oxygen saturation level is placed in the pulse oximeter's optical path. If the wedge (figure 10.4) is moved repetitively back and forth perpendicular to this optical path, either manually or with the aid of a mechanical device, both the pulse rate and shape of the pulse can be altered. Pulse rate can be simulated by changing the frequency at which the wedge is moved across the optical path. The shape of the pulse can be changed by altering the speed at which the wedge is moving.

10.2.1.4 Dual wedge system. In another arrangement of the system, two wedges are used. One is filled with 100% oxygen saturated blood and the other with completely unsaturated blood. The wedges are placed as shown in figure 10.5 and by varying the position along the optical path of this arrangement, virtually any saturation level can be obtained. Note however that with this second arrangement,

MASIMO 2053
Apple v. Masimo APL_MAS_ITC_00015798
IPR2022-01300
RX-0035.0181

an additional external device is needed to obtain a pulsatile variation in the simulator. figure 10.6 shows the polarization filter system proposed by Yount (1989) to achieve this pulsatile variation needed. A pair of polarizing disks simulate the changes in transmittance expected by the pulse oximeter. A stepper motor controls the motion of one disk. This changes the angle of polarization between the two disks, and therefore the amount of light transmitted. By varying the rate of angle change, this system can simulate both the shape and pulse rate seen by the pulse oximeter. This particular system also has several glass windows. This allows for multiple samples to be loaded on the same disk so different oxygen saturation levels can be simulated by rotating the appropriate sample into the probe.

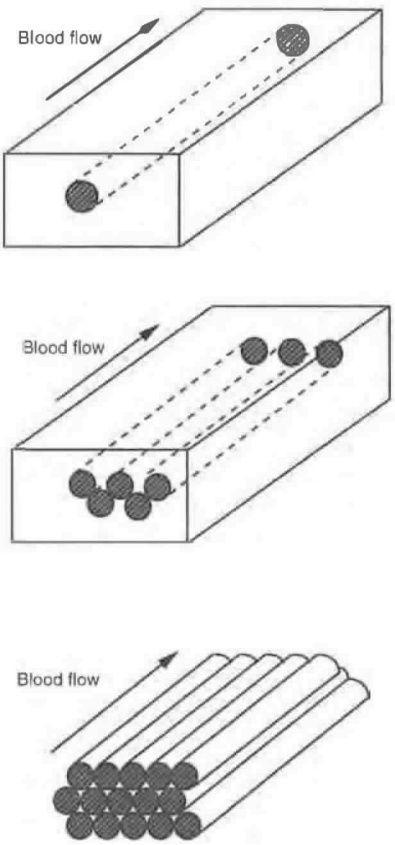

Figure 10.3 Block diagram of various artificial fingers as proposed by Vegfors *et al* (1993).

One limitation of these wedge systems is that if blood is used as the medium in the wedge, the samples either need to be prepared shortly before use or steps need to be taken to stabilize the blood.

MASIMO 2053
Apple v. Masimo
IPR2022-01300
APL_MAS_ITC_00015799
RX-0035.0182

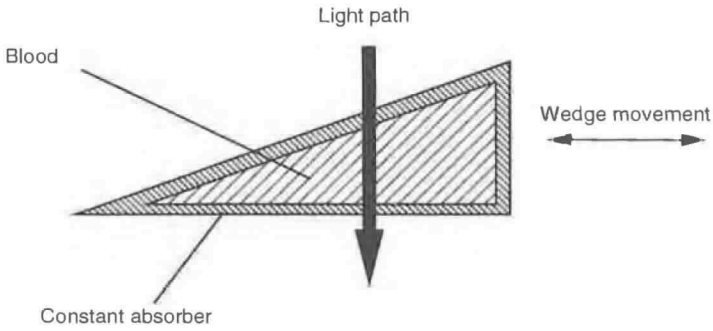

Figure 10.4 Block diagram of a wedge system as proposed by Yount (1989).

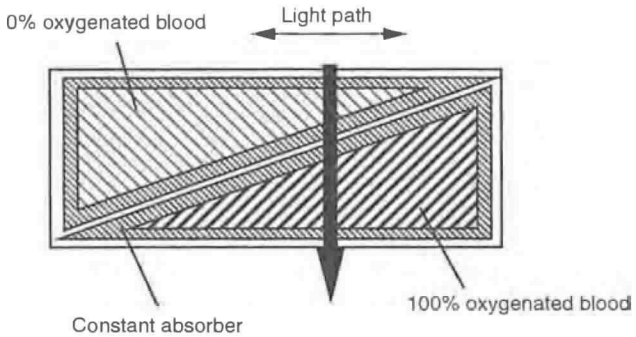

Figure 10.5 Block diagram of the dual wedge system as proposed by Yount (1989).

10.2.1.5 Bulb device. Volgyesi (1989) proposed a simple mechanical design to simulate a pulsing finger. Figure 10.7 shows the tube and bulb type device. It requires a 0.5 to 1 mL blood sample for each saturation level to be tested. A piece of silicone rubber tubing is placed inside a disposable plastic test tube which contains a blood specimen. The operator then manually squeezes the bulb at regular intervals which causes the silicone rubber tubing and the blood in the annular space between the silicone rubber tubing and the test tube to deform or *pulse*. Samples of heparinized blood are externally altered to different saturation levels so different levels of oxygen saturation can be tested. With a variety of oxygen saturation level samples prepared in individual test tubes, the pulse oximeter can be applied to the device. After the operator is able to rhythmically squeeze the bulb for a consistent plethysmograph (rate and amplitude), a reading is recorded from the pulse oximeter and the sample is sent to a CO-oximeter for a comparison reading. The main advantage of this system is its simple implementation. The disadvantage is that the pulsatile nature of the system is operator dependent and samples of known oxygen saturation levels of blood need to be prepared.

MASIMO 2053
Apple v. Masimo
IPR2022-01300
APL_MAS_ITC_00015800
RX-0035.0183

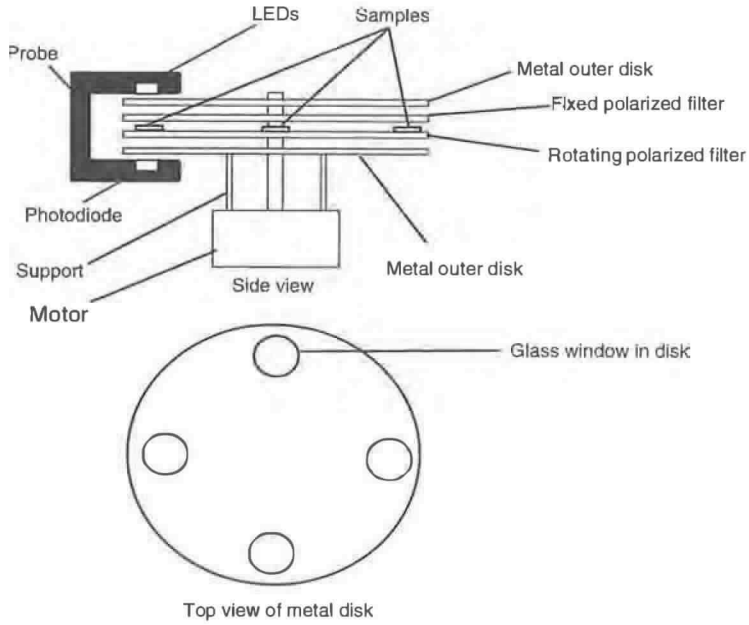

Figure 10.6 Schematic diagram of polarization system (adapted from Yount 1989).

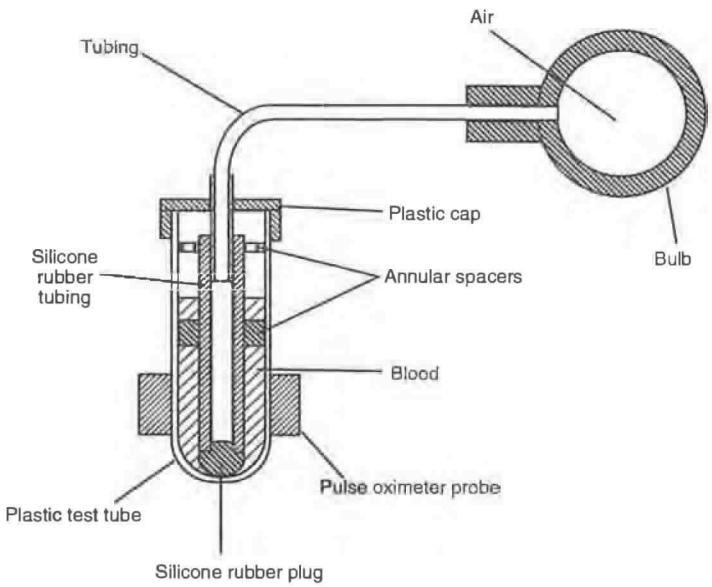

Figure 10.7 Block diagram of tube and bulb device.

MASIMO 2053
Apple v. Masimo
IPR2022-01300
APL_MAS_ITC_00015801
RX-0035.0184

10.2.2 Nonblood simulators

Nonblood simulators, like simulators that use blood, are also based on the concept of being able to simulate the absorbance of human tissue (normally the finger) between the LEDs and the photodiode of the pulse oximeter under test. These devices use colored materials to simulate blood. These simulators use a variety of mechanical and electrical devices to achieve the desired variations in absorbance. The more difficult aspect is simulating the scattering properties of whole blood. One of the most successful studies in this area (Marble *et al* 1994) used a combination of nondairy creamer mixed with solutions of red and green dye.

10.2.2.1 Bulb device. The bulb device described in section 10.2.1 above can also be used with liquids having differing optical absorbance properties corresponding to oxyhemoglobin. A commercial version of this device is currently being marketed by Nonin under the trade name *finger phantom*. This product (Nonin 1995) provides three translucent white *artificial fingers* that simulate arterial blood at nominally 80%, 90%, and 97% saturation levels. The operator gently presses the finger phantom about once every second to generate a pulse. The typical infrared percent modulation when squeezed is 0 to 5%.

10.2.2.2 Wedge device. The wedge device described in section 10.2.1 above can also be used with liquids other than blood having optical absorbance properties corresponding to those of the human finger.

10.2.2.3 Polyester resin device. Figure 10.8 shows a simple test object proposed by Munley *et al* (1989). This device consists of a piece of polyester resin that is formed in the shape of a finger. The resin is adapted to allow a core to be placed inside the artificial finger. At the end of the core, in the area exposed to the pulse oximeter LED's light path, a slotted piece of suitably colored Plexiglas is placed. As the device handle is rotated, the slot allows varying levels of LED light to reach the pulse oximeter photodiode. Speed of rotation of the crank will determine the *pulse rate* that the oximeter reads. Changing the color characteristics of Plexiglas will change the oxygen saturation reading that the pulse oximeter registers. This device was also shown to produce similar oxygen saturation readings among multiple devices of the same make and model of pulse oximeter.

10.2.2.4 Colored colloid simulator. Leuthner (1994) proposed the pulse oximeter development system shown in figure 10.9. A transparent bag is filled with a colored colloid solution. The color determines the extinction coefficients at the two wavelengths of interest. This system uses a water–gelatin mix which is heated and colored with red and black ink. To simulate different oxygen saturation levels, multiple bags with varying ratios of red and black dye need to be prepared. The bag is positioned between two acrylic disks. The disks and bag are then rotated by a stepper motor under microcontroller control. With this configuration, both the DC and AC absorbance ratio can be adjusted. Increasing the angle between the two plates increases change of absorbance over each rotation for an increase in relative AC signal. The simulated pulse shape is determined by speed of the disk rotation and the pulse rate is determined by the rotation frequency. A constant absorber material is placed on top of the disk to simulate the constant light absorbance of fingers of different people. In practice,

MASIMO 2053
Apple v. Masimo
IPR2022-01300
APL_MAS_ITC_00015802
RX-0035.0185

it can vary by a factor of four. Generally a piece of white paper of varying thickness is used as the constant absorber. Two optic fibers are integrated into an artificial finger which then plugs into the finger probe of the pulse oximeter. The other ends of fibers are connected opposite each other near the rotating plates. If testing is done using different waveforms, the angular velocity of the rotation has to change and as such is controlled through the stepper motor via microcontroller control. The whole system is enclosed in a box to prevent disturbances from ambient light.

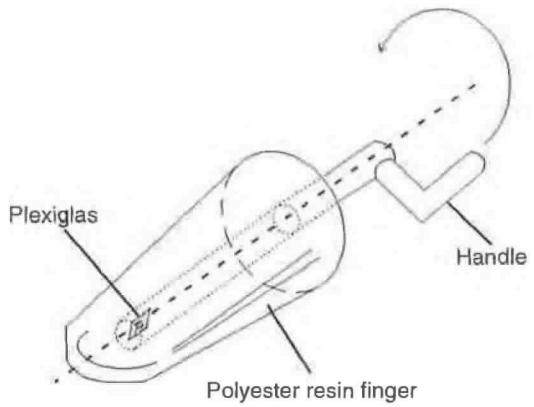

Figure 10.8 Polyester resin system proposed by Munley et al (1989).

The physical behavior of this system can be almost totally described using Beer's law, but the system cannot be used for finding the calibration table of a pulse oximeter. The main reason is that the scattering effect in whole blood is not present in this system. However this system can be used for a rough calibration table of a new instrument and to test an existing pulse oximeter for the response it gives when different colored bags are used.

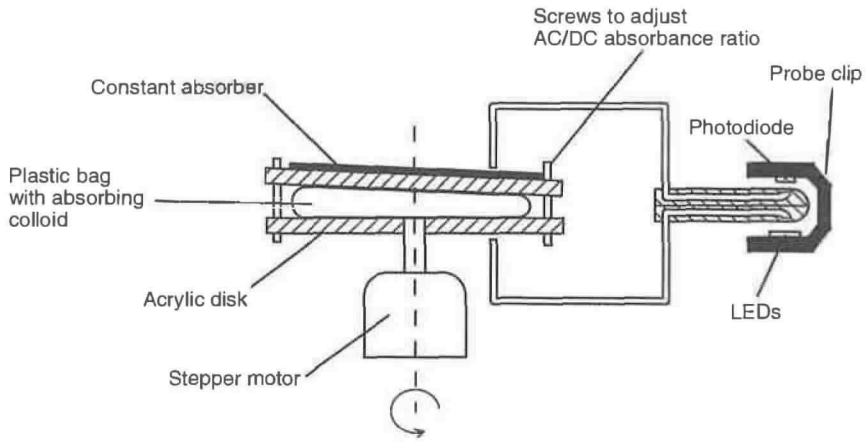

Figure 10.9 Leuthner's (1994) colored colloid disk system.

MASIMO 2053
Apple v. Masimo
IPR2022-01300
APL_MAS_ITC_00015803
RX-0035.0186

10.2.2.5 Liquid crystal retarder simulator. Zhou *et al* (1992) developed a device for generating test signals for pulse oximeters based on a voltage-controlled liquid-crystal light valve. In the first system, the pulse oximeter's LEDs are separated by an optical filter, modulated by a light valve, and recombined before detection by the probe's photodiode. The newer system does not require wavelength separation and its associated hardware as shown in figure 10.10. The transmittance characteristics are varied by taking advantage of the intrinsic wavelength dependence of a twisted-nematic liquid-crystal retarder (LCR). Polarizers are used to generate optical density variations that can be made to resemble blood perfused tissue. The intensity transmitted through the optical system can be adjusted by varying the voltage on the LCR. To simulate a pulsatile change in transmittance, the attenuation is initially made a constant DC value. A small AC voltage is then superimposed on top of the DC voltage to provide a pulsatile component. The transmittance at both the red and IR wavelengths varies depending on the voltage amplitude applied to the LCR. This allows the AC/DC ratios to be controlled by adjusting the amplitude of the voltage applied to the LCR. The polarizers are required because the angle of polarization strongly affects the range of variation of the red/IR ratio and its sensitivity to the applied voltage. Zhou *et al* are continuing work on this concept to provide the capability of simulating the shape of the plethysmographic waveform applied to the LCR.

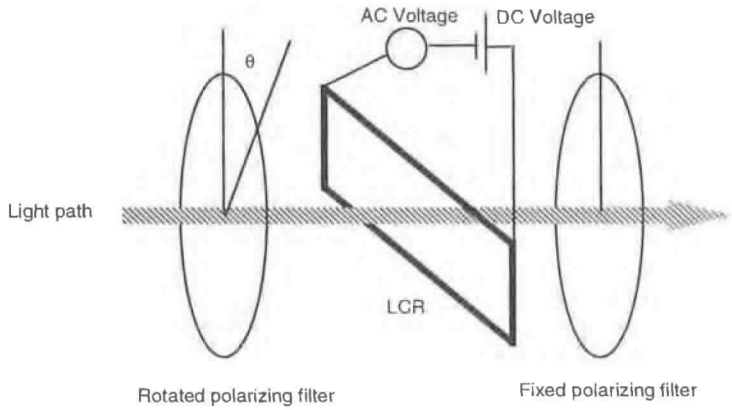

Figure 10.10 Diagram of the liquid crystal retarder (LCR) system proposed by Zhou *et al* (1992).

10.2.2.6 Aoyagi tissue model. A device based on the same general principles as the wedge system been proposed by Aoyagi *et al* (1994). Figure 10.11 shows that a static tissue model having absorption characteristics similar to a human finger is inserted into a pulse oximeter probe. A blood model having blood absorption characteristics similar to a specified oxygen saturation level is moved within the tissue model to simulate pulsatile motion and pulse rate. By altering the geometry of the blood model and/or the rate of motion of the blood model in and out of the tissue model, both the pulsatile waveform and pulse rate can be simulated.

10.2.2.7 Optoelectronic device. A number of relatively simple easy-to-use simulators have begun to appear on the market based on optoelectronic

MASIMO 2053
Apple v. Masimo
IPR2022-01300
APL_MAS_ITC_00015804
RX-0035.0187

principles. Figure 10.12 shows a block diagram for one of these types of simulators. First, the user selects the parameter(s) to be simulated. The pulse oximeter probe is then attached to the device and a signal is received from the pulse oximeter probe's LEDs by the simulator. Pulse separator and timer circuitry convert the red and infrared light pulses from the pulse oximeter probe into electric signals. These signals are modulated with the appropriate level of AC/DC ratio (under computer control) and then converted back to light pulses, via the LED bar, to the probe's photodiode. Finally, the pulse oximeter responds to the converted light pulses as it would to light pulses modulated by living tissue.

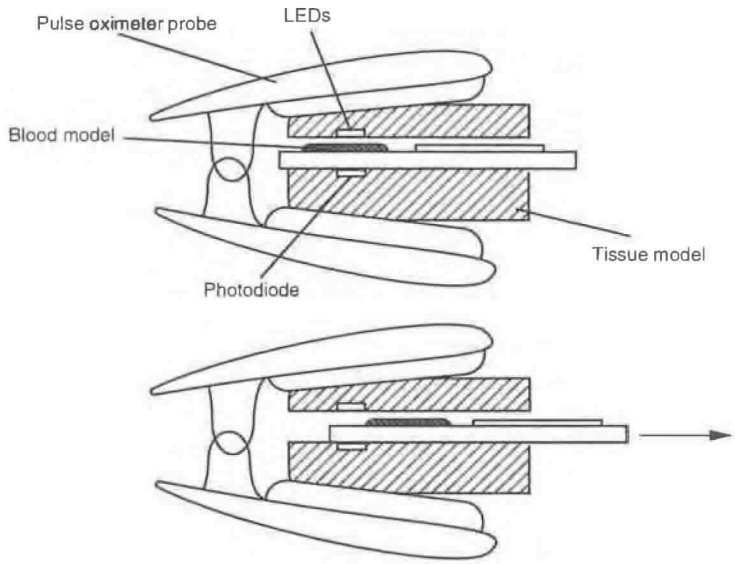

Figure 10.11 Block diagram of system as proposed by Aoyagi *et al* (1994).

These systems can test the probe and oximeter over the complete specified range of the oximeter. Also, simulation of a wide range of conditions is possible. The modulated signal can vary plethysmographic amplitude and wave shape to simulate a variety of ambient light conditions, motion artifacts, and arrhythmias. At least one system (Clinical Dynamics 1995) also includes a probe analyzer capability which independently tests LED and photodiode continuity and sensitivity. These types of simulators are primarily used by pulse oximeter manufacturers during final assembly and checkout of their products. In addition, their capability to generate automatic test sequences help document JCAHO (Joint Commission on Accreditation of Healthcare Organizations) testing requirements.

10.2.3 Electronic simulators

Electronic simulators have limited usefulness since they only simulate electronic signals to and from the probe. Usually these relatively simple devices are provided by the pulse oximeter manufacturer and only check a small number of values. These devices typically plug into the probe port on the pulse oximeter and

MASIMO 2053
Apple v. Masimo
IPR2022-01300
APL_MAS_ITC_00015805
RX-0035.0188

use the drive current of the probe LEDs to generate a simulated photodiode signal back to the pulse oximeter using the device. Figure 10.13 shows an example of such a device. In remote mode, the LEDs just drive an amplifier and the output shows up on the sensor output. This is useful for simple continuity testing. In local mode, these devices are able to electronically simulate a discrete number of simulated oxygen saturation levels, pulse rates and plethysmographic waveform strengths. In addition the calibration resistor value reading capability of the pulse oximeter can be checked. These simulators are good for functional checks of the pulse oximeter's internal circuitry, but because they bypass the pulse oximeter's probe, are of limited usefulness.

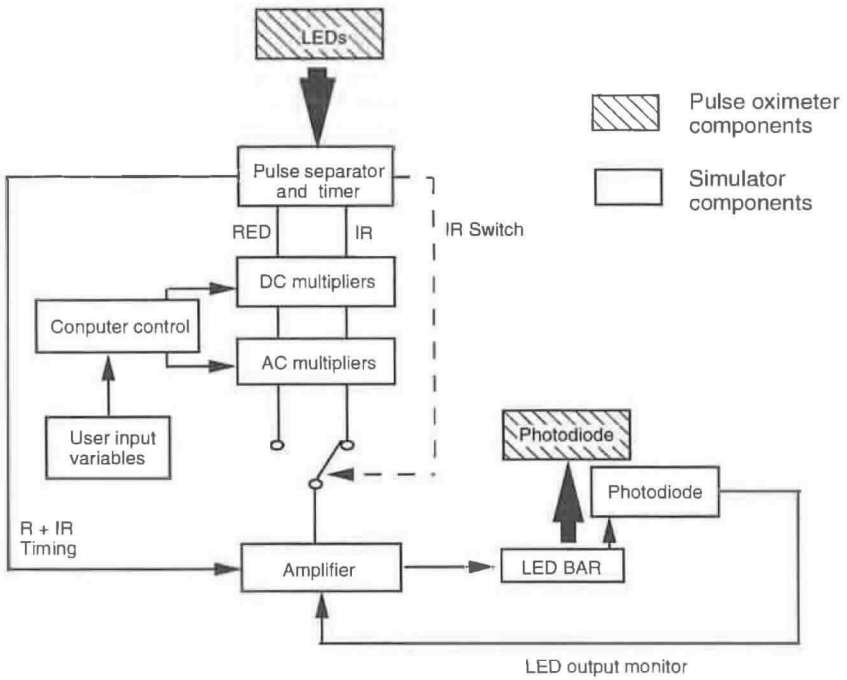

Figure 10.12 Block diagram electro-optic simulator system developed by Merrick and Haas (1994).

10.3 STANDARDS

Although the pulse oximeter has been on the market since 1977 (Santamaria and Williams 1994), surprisingly little standardization has been documented to this point. Statements like 'machines and probes are interchangeable with less than 0.5% difference', 'warm-up time factor of 0.5% to 1.0%' and 'the low perfusion light on the Ohmeda oximeter indicates the oximeter's microprocessor has low confidence level in the data' can be found in the literature. Several standards do exist, but their value from the designer's point of view is limited at best.

MASIMO 2053
Apple v. Masimo
IPR2022-01300
APL_MAS_ITC_00015806
RX-0035.0189

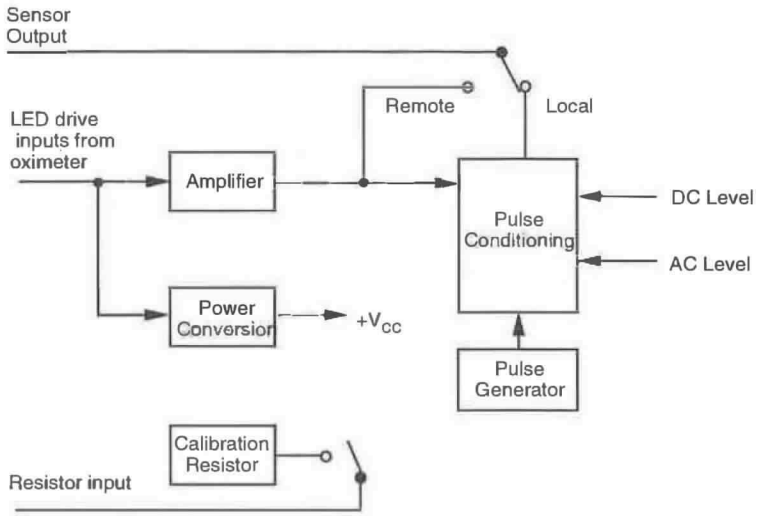

Figure 10.13 Block diagram of an electronic simulator that replaces the pulse oximeter probe (used with permission (Nellcor 1994) Pulse oximeter tester Model SRC-2).

10.3.1 ASTM F1415

The ASTM F1415 standard (ASTM 1992) contains requirements for the pulse oximeter designer in regard to marking and documenting the system, electrical safety concerns, electromagnetic interference and alarms. No specific information is provided regarding specific design requirements of the parts of the system discussed in the preceding chapters. In addition, no specific information is provided in regard to calibration or testing of these devices.

10.3.2 ISO 9919

This standard mentions a few requirements regarding calibration. These include requiring manufacturers to provide:

1. The calibration range of the pulse oximeter.
2. Whether the pulse oximeter is calibrated to display functional or fractional saturation.
3. The accuracy and range of HbO_2 saturation level displayed.
4. Whether the calibration was functional or fractional saturation.
5. Test methods for calibration need to be available from manufacturer upon request.

The ISO 9919 (International Organization for Standardization 1992) also offers this disclaimer in Annex L:

> Values derived from the pulse oximeter are not a measurement of blood or tissue oxygen tension and therefore pulse oximetry provides no direct indication of oxygen delivery to or consumption by, tissues. At present there is no widely accepted direct *in vitro* calibration

MASIMO 2053
Apple v. Masimo
IPR2022-01300
APL_MAS_ITC_00015807
RX-0035.0190

method for pulse oximeters. The only accepted *in vitro* test method for correlation of the reading from a pulse oximeter (S_pO_2) is bench-type oximetry employing more than two wavelengths of light or other methods using blood samples drawn from human subjects. Although work is progressing on the development of direct *in vitro* calibration methods, present techniques still require the use of human subjects. To include test methods in standards that require the use of human subjects, has, through past experience, been found to be unacceptable, and therefore *in vivo* test methods are not included in this International Standard.

10.3.3 Other standards

American Society of Anesthesiologists. Standards for Basic Intra-Operative Monitoring, 1986 (0696-ASA).
American Society of Anesthesiologists. Standards for Post-Anesthesia Care, 1989 (0697-ASA).
European Committee for Standardization. Drafting European norm for pulse oximeters.

REFERENCES

Ackerman S W and Weith P 1995 Knowing your pulse oximetry monitors *Med. Electron.* **26** (1) 82–6
ASTM 1992 *Standard Specification for Pulse Oximeters F1415-92* (Philadelphia PA: American Society for Testing and Materials)
Aoyagi T, Fuse M, Shindo Y and Keto M 1994 Apparatus for calibrating pulse oximeters *US patent 5,278,627*
Cheung P W, Gauglitz K F, Hunsaker S W, Prosser S J, Wagner D O and Smith R E 1993 Apparatus for the automatic calibration of signals employed in oximetry *US patent 5,259,381*
Clinical Dynamics 1995 *Technical sales brochure* (Wallingford, CT: Clinical Dynamics)
International Organization for Standardization 1992 *Pulse Oximeters for Medical Use—Requirements* ISO9919:1992(E)
Leuthner T 1994 Development system for pulse oximetry *Med. Biol. Eng. Comput.* **32** 596–8
Marble D R, Burns D H and Cheung P W 1994 Diffusion-based model of pulse oximetry: *in vitro* and *in vivo* comparison *Appl. Opt.* **33** 1279–85
Merrick E B and Haas P 1994 Simulation for pulse oximeter *US Patent 5,348,005*
Munley A J, Sik M J and Shaw A 1989 A test object for assessing pulse oximeters *Lancet* 1048–9
Nellcor 1994 *Pulse Oximeter Tester Model SRC-2* (Pleasanton, CA: Nellcor)
Nonin Medical 1995 Nonin finger phantom *Technical Note* (Plymouth, MN: Nonin Medical)
Moyle J T B 1994 *Pulse Oximetry* (London: BMG)
Payne J P and Severinghaus J W (eds) 1986 *Pulse Oximetry* (New York: Springer)
Pologe J A 1989 Functional saturation versus fractional saturation: what does the pulse oximeter read *J. Clin. Monit.* **5** 288–9
Reynolds K J, deKock J P, Tarssenko L and Moyle J T B 1991 Temperature dependence of LED and its theoretical effect on pulse oximetry *Brit. J. Anaesthesiol.* **67** 638–43
Reynolds K J, Moyle J T B, Gale L B, Sykes M K and Hahn C E W 1992 *In vitro* performance test system for pulse oximeters *Med. Biol. Eng. Comput.* **30** 629–35
Reynolds K J, Moyle J T B, Sykes M K and Hahn C E W 1993a Responses of 10 pulse oximeters to an in vitro test system *Brit. J. Anaesthesiol.* **68** 265–9
Reynolds K J, Palayiwa E, Moyle J T B, Sykes M K and Hahn C E W 1993b The effects of dyshaemoglobins on pulse oximetry *J. Clin. Monit.* **9** 81–90
Santamaria T and Williams J S 1994 Device focus: pulse oximetry *Med. Device Res. Rep.* **1** (2) 8–10
Severinghaus J W, Naifeh K H and Koh S O 1989 Errors in 14 pulse oximeters during profound hypoxia *J. Clin. Monit.* **5** 72–81
Vegfors M, Lindberg L G, Oberg P A and Lennmarken C 1993 Accuracy of pulse oximetry at various haematocrits and during haemolysis in and in vitro model *Med. Biol Eng. Comput.* **31** 135–41

MASIMO 2053
Apple v. Masimo APL_MAS_ITC_00015808
IPR2022-01300
RX-0035.0191

Volgyesi G A 1992 Method of testing the accuracy of pulse oximeters and device therefor *US patent 5,166,517*
Wukitsch M W, Petterson M T, Tobler D R and Pologe J A 1988 Pulse oximetry: analysis of theory, technology, and practice *J Clin. Monit.* **4** 290–301
Yount J E 1989 Device and procedures for in vitro calibration of pulse oximetry monitors *US patent 4,834,532*
Zhou G X, Schmitt J M and Walker E C 1992 Electro-optical simulator for pulse oximeters *Med. Biol. Eng. Comput.* **31** 534–9

INSTRUCTIONAL OBJECTIVES

10.1 Describe how R curves are determined through *in vivo* testing.
10.2 Explain the role that LED temperature plays in oxygen saturation level determination.
10.3 Explain why the term S_pO_2 is necessary when referring to oxygen saturation levels.
10.4 Explain the reason why different R curves may be needed for a manufacturer's pulse oximeter system.
10.5 Describe how oxygen saturation level is altered through an *in vitro* test system.
10.6 Explain why pulse oximeters are less accurate for S_pO_2 saturation levels below 60%.
10.7 Describe the operation of an optoelectronic simulator system.
10.8 Describe the operation of an colored colloid simulator system.
10.9 Describe the operation of polyester resin device simulator system.
10.10 Describe the operation of a wedge simulator system.
10.11 Describe the operation of the tube and bulb simulator system.
10.12 Explain the limitations of the electronic simulators used for testing pulse oximeters.

MASIMO 2053
Apple v. Masimo
IPR2022-01300
APL_MAS_ITC_00015809
RX-0035.0192

CHAPTER 11

ACCURACY AND ERRORS

Supan Tungjitkusolmun

Continuous assessment of arterial oxygen saturation (S_aO_2) is important in clinical management of critically ill patients. Pulse oximeters have been widely used as blood oxygen monitoring devices since the early 1980s. Currently, pulse oximeters can be found in virtually every operating room, recovery room, and intensive care unit. The advantages of pulse oximetry include noninvasiveness, ease of use, portability, and patient comfort. A light source generated by two LEDs, with wavelengths at approximately 660 nm and 940 nm, and a photodiode are mounted in a probe of a pulse oximeter. Circuit control, saturation calculation, and display are managed by a microprocessor instrument as described in chapter 8. Unlike earlier techniques such as the *in vivo* eight-wavelength oximeter (chapter 3), no heating or arterialization techniques are required in pulse oximetry.

All pulse oximeters work using absorption spectrophotometry, however, considerable differences exist in the way different manufacturers obtain and process the data. These differences occur in the light-emitting diodes, sampling frequency, microprocessor algorithms, and the constants used in the calculations, or the look-up tables. Since the technique has come into wide clinical use over the past decade, it is important to examine circumstances where its reliability may be questioned. The objective of this chapter is to describe several sources of error in pulse oximetry which may cause hazardous consequences to the patients. Recognizing the limitations described in this chapter and applying appropriate corrective interventions are essential to optimize the clinical use of pulse oximeters.

11.1 EVALUATION OF PULSE OXIMETERS

The *gold standard* measurement of arterial oxygen saturation is the CO-oximeter, described in chapter 3. A comparison of the pulse oximeters' readings and CO-oximeters' readings is thus required to verify the reliability of the pulse oximetry technique. Comparisons between pulse oximeters' arterial oxygen saturation values and the CO-oximeters' readings, as well as the HP eight-wavelength ear oximeter will be discussed in this section.

MASIMO 2053
Apple v. Masimo
IPR2022-01300
APL_MAS_ITC_00015810
RX-0035.0193

11.1.1 Accuracy, bias, precision, and confidence limit

Accuracy is a measure of systemic error or bias; the greater the error, the less accurate the variable. The accuracy of a measurement is the degree to which it actually represents what it is intended to represent. The location of the mean errors reflects the accuracy of the measurement. The accuracy of pulse oximeter oxygen saturations can usually be tested by comparing with the reference techique, CO-oximetry. Parameters frequently used to represent the degree of accuracy are bias, and absolute mean errors. *Bias,* in this case, is defined as the mean of the differences between the pulse oximeter readings and the CO-oximeter readings, which can be expressed as

$$\text{bias} = \frac{\sum_{i=1}^{N} x_i}{N} = \bar{x} \tag{11.1}$$

where x_i is calculated by subtracting the ith CO-oximeter measurement from the corresponding oximeter saturation displayed by a pulse oximeter. N is the total number of measurements. Units are percent saturation.

Precision is a measure of variation of random error, or degree of reproducibility. The dispersion of points around the mean reflects the precision of the measurement. Precision is often described statistically using the standard deviation (SD) of the differences between the pulse oximeter readings and the CO-oximeter readings of repeated measurements (Nickerson *et al* 1988) as in equation (11.2). Units are percent saturation.

$$\text{precision} = \text{SD} = \sqrt{\frac{\sum_{i=1}^{N} (x_i - \bar{x})^2}{N-1}}. \tag{11.2}$$

Some researchers frequently use a *95% confidence limit,* which for a normal distribution is equal to 1.96 times SD:

$$95\% \text{ confidence limit} = 1.96 \times \text{SD} \approx 2 \times \text{SD}. \tag{11.3}$$

Example 1

The results from an experiment to compare pulse oximeter and CO-oximeter readings are shown in table 11.1. Ten measurements were made.

From table 11.1,

$$\text{bias} = \bar{x} = \frac{\sum_{i=1}^{10} x_i}{10} = \frac{15}{10} = 1.5\%$$

MASIMO 2053
Apple v. Masimo
IPR2022-01300
APL_MAS_ITC_00015811
RX-0035.0194

$$\text{precision} = \sqrt{\frac{\sum_{i=1}^{10}(x_i - \bar{x})^2}{10-1}} = \sqrt{\frac{20.5}{9}} = 1.51\%,$$

Table 11.1 Comparison of pulse oximeter and CO-oximeter readings.

Measurement (i)	CO-oximeter readings (%)	Pulse oximeter readings (%)	x_i (%)	$x_i - \bar{x}$
1	97	100	3	1.5
2	98	99	1	−0.5
3	92	91	−1	−2.5
4	96	98	2	0.5
5	97	99	2	0.5
6	90	93	3	1.5
7	89	90	1	−0.5
8	95	98	3	1.5
9	88	90	2	0.5
10	93	92	−1	−2.5

and

$$95\%\text{ confidence limit} \approx 2 \times 1.51\% = 3.02\%.$$

The bias of 1.5% means that the test pulse oximeter tends to *overestimate* the oxygen saturation level (postive bias). A 95% confidence limit of 3.02% means that the pulse oximeter will give an outcome in the range between 1.5 − 3.02% and 1.5% + 3.02%, or between −1.52% and 4.52% from the true value (the CO-oximeter reading) with a probability of 0.95.

The use of bias and precision is helpful in getting a clear picture of a pulse oximeter's performance and how this compares to other units or other studies. A unit may be very precise, so that the results are highly reproducible with a low scatter, but have a high bias so that the results are not centered on the true values. In contrast, a unit may have a very low bias, but have poor precision, with values swinging widely from side to side of the true value. In clinical practice, a 95% confidence limit of less than ±3% is considered acceptable for most cases.

Other statistical terms from the regression analysis (correlation coefficient, positive error, intercept, and slope) are also used in several studies (Yelderman and New 1983, Taylor and Whitwam 1988).

11.1.2 What do pulse oximeters really measure?

Pulse oximeters only measure a ratio of transmitted red and infrared light intensities, and relate this to a look-up table of empirical oxygen saturation values (see chapter 9). The values in the table depend on the manufacturer's purpose of estimating functional or fractional oxygen saturation, but will in reality be neither of these unless the dyshemoglobin (dysfunctional hemoglobin) levels, and the pH levels in a subject's arterial blood are exactly the same as the average values of those used in the empirical calibration to create the look-up table. Choe *et al* (1989) found that the measured oxygen saturations in two instruments (Ohmeda Biox 3700 and Radiometer Pulse Oximeter) were close to the fractional oxygen saturation (fractional SO_2). On the other hand, the other four units used in the study (Minolta/Marquest Pulsox 7, Novametrix 500, Physio-Control Lifestat, and Datex Satlite) gave results in the proximity of functional oxygen

MASIMO 2053
Apple v. Masimo
IPR2022-01300
APL_MAS_ITC_00015812
RX-0035.0195

saturation (functional SO_2). The data used for calibration processes are usually obtained from healthy adults breathing hypoxic gas mixtures (see section 10.1.1).

Pulse oximeters can measure neither fractional SO_2 nor functional SO_2. However, the use of fractional SO_2 as the reference in the calibration process provides the clinician with a realistic assessment of the magnitude of the errors of physiological illness which is likely to be found for the group of patients under consideration.

11.1.3 Pulse oximeter versus CO-oximeter

Pulse oximeters are empirically calibrated by the manufacturer against a CO-oximeter. The IL (Instrumentation Laboratories, Inc.) 482 and 282 model CO-oximeters use four wavelengths of light (535.0, 585.2, 594.5, 626.6 nm) to detect the concentrations of HbO_2, Hb, COHb, and MetHb, and give the oxygen saturation as a percentage of the sum of the four species. This saturation is known as *fractional saturation* (section 4.2.2).

According to its operator's manual, the IL 482 has a precision of 0.5% (95% confidence limit of 1%) for HbO_2 measurements for samples with 0 to 10% MetHb and a pH of 7.0 to 7.4. The pH sensitivity of MetHb can cause significant changes in absorption at all four wavelengths outside these MetHb and pH ranges. Accuracy is also compromised by the presence of high lipid levels which can cause light scattering. It is not feasible to validate the value of 0.5% precision claim, since there is no quality control sample of accurately known or measured saturation that can be used to verify this. It is reasonable to accept this precision, given the high degree of reproducibility of the results.

Yelderman and New (1983) conducted a study to evaluate the accuracy of pulse oximeters over a broad range of arterial blood oxygen saturation in 1983 when the first Nellcor pulse oximeter became commercially available. A comparison of a pulse oximeter and the CO-oximeter readings was performed on five healthy, nonsmoking students ranging in age from 18 to 25. The precision of the measurements was found to be 1.83%. They concluded that pulse oximetry is a reliable technique for a measurement of arterial blood oxygen saturation in the range of 100 to 70%.

11.1.4 Pulse oximeter versus in vivo eight-wavelength ear oximeter

Hewlett-Packard ear oximetry, using eight wavelengths, was considered as a standard technique of measurement of arterial oxygen saturation before pulse oximeters were invented (see chapter 3). A comparison of the two techniques is thus necessary to see whether their results agree sufficiently for the pulse oximeter to replace the previous technique. Cahan *et al* (1990) determined that the difference between the HP ear oximeter (Hewlett-Packard 47201A ear oximeter) and the CO-oximeter (IL 282) readings was 0.9 ±4.3% (expressed as bias ± 95% confidence limit).

In a study by Cahan *et al* (1990), the difference between the individual pulse oximeters and the HP ear oximeters was found to be 2.6 ± 10.3% in the range of 99 to 70%. All five pulse oximeters studied gave higher values than the HP oximeter, and the differences between pulse oximeters and the HP readings increased as oxygen saturation fell below 85%. The greater discrepancies might be due to the longer *delay* of pulse oximeters during the progressive hypoxia.

MASIMO 2053
Apple v. Masimo
IPR2022-01300
APL_MAS_ITC_00015813
RX-0035.0196

The agreement of discrete measurements of the two methods was found to be acceptable at high oxygen saturation but unacceptable for arterial oxygen saturation levels lower than 85%. We must be careful when making an assessment of the oxygen saturation levels from two experiments in which different arterial oxygen monitoring devices were used. The continuous measurements from pulse oximeters and from the HP ear oximeters cannot be assumed to be in the same range.

11.2 ACCURACY VERSUS SATURATION

Accuracy at different levels of oxygen saturation is not the same. To make the discussion more effective, oxygen saturation is divided into three ranges: normal saturation, high saturation, and hypoxic condition (low saturation level).

11.2.1 High saturation (greater than 97.5%)

Pulse oximeters are designed to give a saturation reading of less than or equal to 100%; this limits the potential for positive errors and makes precision calculations difficult to interpret in this high range. Table 11.2 offers some outcomes of the evaluations of 20 brands of pulse oximeters. Even though precision calculations cannot be determined unbiasedly due to positive errors, the correct corresponding oxygen saturation is not critical in this range. As long as the oxygen saturation is over 97%, the patients are in favorable conditions and they require no urgent medical attention.

Table 11.2 Number of S_pO_2 readings of 100% when CO-oximeter reading was 97 to 98%. The results are expressed as the ratio of S_pO_2 readings of 100% and the number of measurements (percentage). Adapted from Webb *et al* (1991). Study 1 is from ECRI (1989). Study 2 is from Clayton *et al* (1991a).

Oximeter	Study 1	Study 2
Criticare CSI 503	–	0/17 (0%)
Engstrom EOS	–	0/15 (0%)
Spectramed Pulsat	0/17 (0%)	0/15 (0%)
Criticare CSI 504	–	0/14 (0%)
Biochem Microspan 3040	–	0/10 (0%)
Radiometer Oximeter	1/11 (9%)	1/17 (6%)
Simed S-100	1/17 (6%)	1/15 (0%)
Invivo 4500	2/9 (22%)	2/15 (13%)
Datex Satlite	1/9 (11%)	3/22 (14%)
Datascope Accusat	4/9 (44%)	3/14 (21%)
Physio-Control 1600	2/17 (12%)	4/16 (25%)
Nonin 8604D	3/9 (33%)	4/16 (25%)
Sensormedics Oxyshutle	2/7 (29%)	6/16 (38%)
Novametrix 505	3/17 (18%)	11/22 (50%)
Pulsemate Colin BX-5	–	10/16 (63%)
Minolta Pulsox 7	–	11/17 (65%)
Ohmeda Biox 3700	4/9 (44%)	11/15 (73%)
Ohmeda Biox 3740	5/16 (31%)	13/16 (81%)
Nellcor N-200	3/17 (18%)	13/18 (83%)
Kontron 7840	–	13/15 (87%)

MASIMO 2053
Apple v. Masimo APL_MAS_ITC_00015814
IPR2022-01300
RX-0035.0197

11.2.2 Normal saturation (90 to 97.5%)

After more than a decade of development since first becoming commercially available, most models of pulse oximeters have a reliable performance in this range. In an experiment by Webb *et al* (1991), 10 of the 13 units had absolute mean errors of less than 1.0%; the standard deviation was less than 2% in eight units, and between 2 and 3% in the remaining five. Choe *et al* (1989), Taylor and Whitwam (1988), and Yelderman and New (1983) also found similar results. Pulse oximeters are well calibrated in this range since it is the most commonly found condition.

11.2.3 Low saturation (less than 80%)

Pulse oximeters have a high potential for errors at low saturations, mainly because ethically manufacturers cannot induce severe hypoxia repeatedly in volunteers for calibration purposes. Also, figure 11.1 illustrates that the absorption characteristics of 0% oxygen saturation blood are much steeper than that of 100% oxygen saturation blood at a 660 nm wavelength. At this range, when the percentage of hemoglobin saturation decreases, the slope of the absorption spectrum increases. Any slight error in the LED peak wavelength will change the readings of the pulse oximeter drastically.

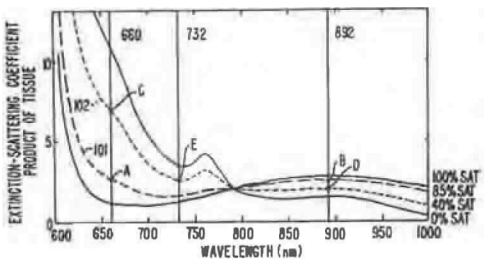

Figure 11.1 Variation in extinction coefficients over a range of wavelengths of 600 to 1000 nm at different saturation values. At 660 nm (red) wavelength, the slope of an absorption spectrum increases as oxygen saturation level decreases. From Casciani *et al* (1995).

The error associated with low saturations can also be explained by a reduction in the signal-to-noise ratio in pulse oximetry. As saturation decreases, less red light is able to penetrate through the tissues due to a high absorbance of Hb, thus the AC signal becomes weaker. To compensate for this drawback, the LED-driving current and the photodiode amplifier gain are increased to maintain the AC signal in a usable range. As the gain increases, incidental electrical and physiological noise also increase, thus resulting in a decline in the pulse oximeter's accuracy.

The accuracy of 13 pulse oximeters at low saturations was determined by ECRI (1989) in intensive care patients. Figure 11.3 shows the experimental results. All units examined were less accurate and nine out of 13 were less precise than when saturations were greater than 80%; eight out of 13 units tended to underestimate S_aO_2 by substantial amounts at low saturations.

In summary, pulse oximeters are poorly calibrated for saturations below 80%. In general, accuracy and precision are worse than for saturations above

MASIMO 2053
Apple v. Masimo
IPR2022-01300
APL_MAS_ITC_00015815
RX-0035.0198

80%, but this depends on the model and the brand. For example, Sensormedics Oxyshuttle pulse oximeter's bias only increases slightly (−0.1%), and the precisions are the same in both ranges.

Table 11.3 Accuracy of 13 pulse oximeters using finger probes on patients in the Intensive Care Unit. Adapted from Webb *et al* (1991).

Oximeter	Saturation > 80% Bias% (precision%)	Saturation < 80% Bias% (precision%)
Datascope Accusat	−0.3 (1.9)	−7.1 (3.2)
Datex Satlite	+0.0 (2.0)	+1.4 (1.5)
Invivo 4500	−0.3 (1.8)	−0.6 (4.9)
Nellcor N-200	+0.8 (1.7)	−5.5 (3.5)
Nonin 8604	+1.4 (1.8)	+8.8 (4.8)
Novametrix 505	+0.7 (1.9)	−8.1 (4.3)
Ohmeda 3700	−1.0 (2.5)	−5.3 (6.2)
Ohmeda 3740	−0.1 (2.8)	−5.5 (1.9)
Physio-Control 1600	+0.0 (1.9)	−6.0 (6.9)
Radiometer Oximeter	−1.5 (1.8)	−6.7 (3.2)
Sensormedics Oxyshuttle	−0.3 (1.8)	−0.4 (1.8)
Simed S-100	+0.1 (2.2)	+1.8 (1.6)
Spectramed Pulsat	+0.7 (1.6)	−3.4 (3.2)

11.3 ACCURACY VERSUS PERFUSION

Pulse oximeters require adequate plethysmographic (photoplethysmographic) pulsations to differentiate arterial blood absorbance from the absorbances of other substances (venous blood, tissue, and bone). A significant decrease in peripheral vascular pulsation, such as in hypothermia, vasoconstriction, hypotension, during cardiopulmonary bypass, or cardiac arrest, may result in a plethysmographic signal insufficient to be processed reliably by the oximeter. Most pulse oximeters have the ability to recognize a weak waveform which could cause an erroneous reading. They usually display a '*Low Perfusion*' or similar message to alert the user of possible problems in peripheral blood perfusion.

In a study to compare the performance of 20 pulse oximeters under the conditions of poor perfusion by Clayton *et al* (1991a), only two out of 20 oximeters had 95% confidence limits that were less than 4%. Generally the clinically acceptable range for the readings is about ±3%. Table 11.4 shows the results from the experiment.

Locally applied vasodilating drugs could be useful to enhance the plethysmographic pulsation in certain situations. The use of a pediatric warming blanket wrapped around the forearm is a simple method to increase perfusion due to a cold finger if the pulse oximeter signal is weak. Finger probes are preferable for patients with poor perfusion (see section 11.9).

11.3.1 Venous congestion

Another potential problem with pulse oximeter measurements is venous congestion, which leads to artifacts due to venous pulsation. Venous congestion is an accumulation of blood within an organ, which is the result of back pressure within its veins. Because the pulse volume amplitude of the plethysmograph is a measure of the pulsatility of the compliant vessels, some of the pulse may be

MASIMO 2053
Apple v. Masimo APL_MAS_ITC_00015816
IPR2022-01300
RX-0035.0199

attributed to venous blood of lower oxygen content mixed with the signal due to higher oxygen content in the arterial blood. Also, the decrease in venous wall compliance by congestion should decrease the pulse volume amplitude in the organs (such as the finger). The pulse oximeter is unable to distinguish between the absorption due to pulsatile veins and that caused by arteries and arterioles. Pulsatile venous flow is generated by a transmitted arterial pulse through *arteriovenous anastomoses* in the finger. Therefore, if the S_pO_2 measured by the pulse oximeter is shunted arterial blood in the vein, the S_pO_2 reading will be affected by venous blood. Pulsatile veins may lead to the pulse oximeter indicating a lower value of S_pO_2 than is the actual saturation.

Table 11.4 Accuracy of pulse oximeters, ranked according to number of readings within 3% and showing ranking for number of readings within 3% of total number of readings expressed as percentage. Each pulse oximeter was tested on 40 patients. Total = total number of measurements obtained. Adapted from Clayton *et al* (1991a).

Pulse oximeter	Total	# within ±3%	Percent ±3%/Total	Rank
Criticare CSI 503	40	40	100	1
Datex Satlite	40	38	95	2
Biochem Microspan 3040	28	26	93	3
Novametrix 505	38	35	92	4
Criticare CSI 504	39	35	90	5
Invivo 4500	38	34	89	6
Sensormedics Oxyshuttle	36	32	89	6
Physio-Control 1600	36	31	89	6
Ohmeda Biox 3740	30	26	87	9
Minolta Pulsox 7	40	34	85	10
Nellcor N-200	39	33	85	10
Simed S-100	36	30	83	12
Datascope Accusat	33	27	82	13
Radiometer Oximeter	40	32	80	14
Nonin 8604D	35	28	80	14
Spectramed Pulsat	32	25	78	16
Pulsemate Colin BX-5	39	30	77	17
Ohmeda Biox 3700	36	25	69	18
Kontron 7840	40	27	68	19
Engstrom Eos	35	20	57	20

Much of the ac display of the plethysmographic signal may be due to pulsatile cutaneous venules which have an oxygen saturation similar to the arterial saturation due to patient arteriovenous communications in the skin. However, if the large venules and veins, which carry hemoglobin with a lower oxygen saturation, are pulsating, then the technique cannot distinguish between the two. Therefore, the S_pO_2 values may be lower than the arterial oxygen saturation if venous congestion is present. Other causes of increased pulsatility in veins are arteriovenous disassociation, right atrial myxoma, and right heart block.

11.4 ACCURACY VERSUS MOTION ARTIFACTS

As with most medical devices, motion artifacts contribute a significant error to pulse oximetry. Pulse oximeters detect a pulsatile signal that normally is only a small percentage of the total plethysmographic signal. Therefore, any transient motion of the sensor relative to the skin can cause a significant artifact in the

MASIMO 2053
Apple v. Masimo
IPR2022-01300
APL_MAS_ITC_00015817
RX-0035.0200

optical measurement. Furthermore, if these transient artifacts mimic a heartbeat, the instrument may be unable to differentiate between the pulsations that are due to motion artifacts and normal arterial pulsations, thereby causing erroneous readings. Practically, these artifacts can be reduced by digital signal processing and averaging the S_pO_2 values over several seconds before they are displayed. Motion artifacts, such as during shivering, seizure activity, or exercise, are usually recognized by false or erratic heart-rate displays or by distorted plethysmographic waveforms (figure 11.2).

Some manufacturers use the R wave of the patient's electrocardiogram to synchronize the optical measurements; they thereby improve the detection of noisy pulsatile signals by enhancing the signal-to-noise ratio of the measurements through the use of multiple time-averaged signals (see chapter 9).

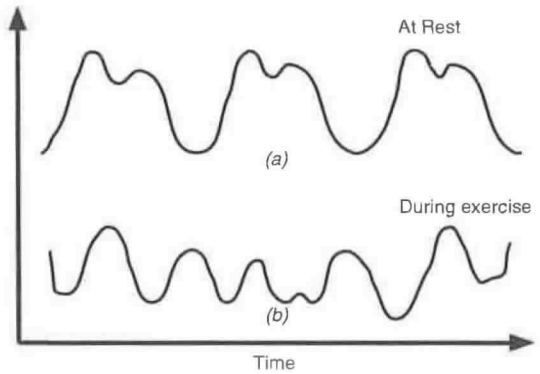

Figure 11.2 The plethysmographic waveform of a subject at rest is periodic (*a*) and during exercise is not periodic (*b*).

11.5 ACCURACY VERSUS OPTICAL INTERFERENCE

Bright external light sources are known to affect pulse oximeters and all pulse oximeters share this sensitivity. This occurs because these instruments use optical means to make their measurements. Consequently, to obtain accurate measurements, potential sources of optical interference must be controlled. Because pulse oximeters' optical components are located in the probe, proper probe application and use are key factors in reducing optical interference. Optical interference occurs when bright light from an external source (ambient light) reaches the photodiode, or when light reaches the photodiode without passing through a pulsatile arteriolar bed.

Pulse oximeters are designed to reject ambient light since the photodiodes can measure weak signals. When the intensity of ambient light is high (as from heat lamps or sunlight), the photodiode cannot sense light transmitted through tissue for S_pO_2 calculations. Protecting the photodiode from bright light obviates the problem. One solution is to cover the probe site with some opaque material, such as a surgical towel. Although this approach is generally useful, with active neonates or restless patients, the towel frequently becomes displaced and exposes the oximeter probe. One of the effective remedies to this problem is covering the

MASIMO 2053
Apple v. Masimo
IPR2022-01300
APL_MAS_ITC_00015818
RX-0035.0201

probe, while it is attached to a digit, with a packaging from an alcohol swab as suggested by Siegel and Gravenstein (1987). This packaging is manufactured in a shape that makes a convenient, dark receptacle for a digit, even one on which a flexible pulse oximeter probe has been placed.

Another type of optical interference may occur when some of the light from the LEDs reaches the photodiode without passing through an arteriolar bed. Such an optical shunt results in either erratic or stable but inaccurate measurements. Figure 11.3 shows some optical interferences to pulse oximetry. Oximeter probes should be manufactured of black opaque material that does not transmit light, or enclosed in an opaque plastic housing. Although there is no substitute for continual vigilance, shielding the probes from excessive ambient light, as strongly recommended by the manufacturer, will reduce the possibility of false readings.

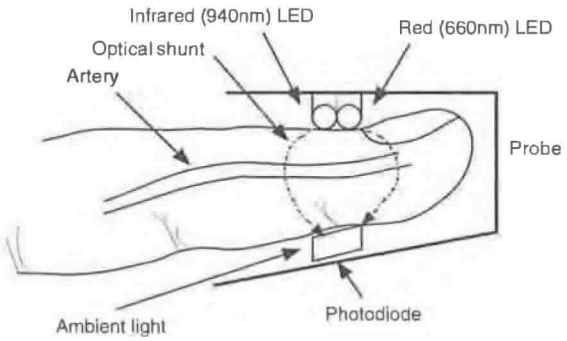

Figure 11.3 Ambient light interference and optical shunt in pulse oximetry. Optical shunt occurs when the light from the LEDs reaches the photodiode without passing through arterial blood.

11.6 ACCURACY VERSUS INTRAVENOUS DYES

During medical procedures, the use of substances such as dyes may be necessary. This section investigates the effects of dyes on pulse oximeter readings.

Several intravenous-administered dyes appeared to be associated with abrupt decreases in pulse oximetry S_pO_2 readings (Scheller *et al* 1986). Fifteen white subjects were studied, five with each of the three dyes, indigo carmine (InCa), indocyanine green (InGr), and methylene blue (MeBl). In all subjects, baseline readings were 97% or greater in both the toe and finger locations. Table 11.5 summarizes subject characteristics, the time from injection to the first noticeable decrease in S_pO_2 readings (latency), the lowest S_pO_2 reading (nadir), and the time required to return to baseline (duration), for each of the three dyes. Of the three dyes, InCa produced the fewest and smallest changes in S_pO_2 readings. Decreases from baseline were observed in three of the five subjects given indigo carmine, but only in the toe location. The magnitude of the measured oxygen saturation decreases were small following InCa, and the lowest S_pO_2 reading observed in any subject was 92%. By contrast, oxygen saturation reading decreases were observed in all subjects in both sensing locations following the administration of MeBl, with a median lowest S_pO_2 reading of 65%. The lowest S_pO_2 reading observed in any subject following MeBl was 1%. In subjects given

MASIMO 2053
Apple v. Masimo APL_MAS_ITC_00015819
IPR2022-01300
RX-0035.0202

MeBl, measured oxygen saturations remained below baseline for between approximately 1 and 2 min in both the finger and toe. S_pO_2 reading decreases following the administration of InGr were intermediate between those observed with MeBl and InCa. Figure 11.4 shows the absorbance spectra for the three dyes as determined by spectrophotometry.

Table 11.5 Subject characteristics and S_pO_2 reading responses to IV Dyes. Adapted from Scheller *et al* (1986). Latency = the time from injection to the first noticeable decrease in S_pO_2 readings. Nadir = the lowest S_pO_2 reading. Duration = the time required to return to baseline reading. NC = no observed change.

Dye	Weight (kg)	Height (cm)	Latency (s) Finger/Toe	Duration (s) Finger/Toe	Nadir (O_2 saturation, %) Finger/Toe
MeBl	75	178	80/65	70/90	91/98
	68	175	35/30	105/80	58/65
	79	183	40/40	65/50	76/59
	93	180	40/35	50/50	80/69
	46	163	35/30	115/80	1/32
InGr	83	188	35/45	10/40	96/96
	67	175	45/40	35/25	95/93
	70	178	45/35	45/70	93/84
	86	191	50/45	70/30	93/92
	70	175	NC/65	NC/60	99/88
InCa	83	188	NC/NC	NC/NC	NC/NC
	67	178	NC/40	NC/40	NC/93
	46	163	NC/25	NC/30	NC/92
	86	175	NC/NC	NC/NC	NC/NC
	65	173	NC/20	NC/20	NC/94

All the three dyes absorb light in the region of the 660 nm wavelength at which the red LED of a pulse oximeter emitted light. Methylene blue has an extremely high absorbance in this region. This explains why methylene blue interferes to a greater degree with S_pO_2 readings than the other dyes (from Beer's law). Likewise, the absorbance of indocyanine green is slightly greater than indigo carmine at this wavelength, which is consistent with the observation that S_pO_2 readings were affected to a greater degree in those subjects given indocyanine green than in those given indigo carmine.

Absorbances of all three dyes are negligible in the region of 940 nm and thus have insignificant effects on the IR light intensities detected by photodiodes. The variable responses of the individual subject's S_pO_2 readings following dye injection may have been related to differences in cardiac output or blood volume. For example, following methylene blue, the largest S_pO_2 reading decrease and longest duration of decrease was seen in the smallest subject (body surface area = 1.34 m^2). The measurement of cardiac output by the transcutaneous detection of various intravenous dyes has been studied in both adults and children and found to correlate well with dye dilution methods that use continuous arterial blood sampling (Scheller *et al* 1986).

Saito *et al* (1995) observed that after intra-arterial injection of the blue dye *patent blue* in an anemic patient, the reduction in the pulse oximeter readings sustained for more than 20 min.

MASIMO 2053
Apple v. Masimo
IPR2022-01300
APL_MAS_ITC_00015820
RX-0035.0203

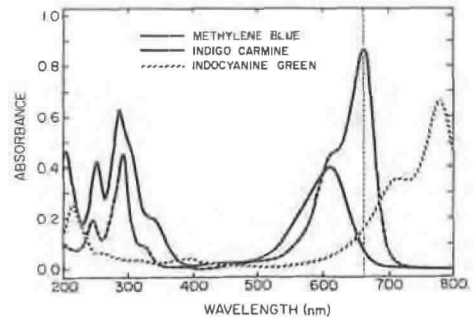

Figure 11.4 Absorbances of dyes. MeBl has the highest absorbance in the region of the 660 nm wavelength. From Scheller (1986).

Clinicians should be aware of the potential influences of intravenously administered dyes on S_pO_2 monitor readings so that operating room time is not wasted and more invasive analysis not undertaken, e.g., arterial blood gases, should falsely low S_pO_2 readings be temporarily induced by administration of these dyes (Scheller *et al* 1986).

11.7 EFFECT OF DYSHEMOGLOBINS AND FETAL HEMOGLOBIN

Dyshemoglobins are abnormal hemoglobins which cannot transport oxygen to the tissues. The presence of dyshemoglobins may cause inaccuracy in pulse oximetry. This section will discuss the two most commonly found in adults, carboxyhemoglobin and methemoglobin, as well as fetal hemoglobin.

11.7.1 Carboxyhemoglobin (COHb)

Seidler *et al* (1993) observed limitations of S_pO_2 readings in patients treated after inhalation of CO. Serial measurements of COHb concentration (IL 482 CO-oximeter) were done hourly in 6 patients until the results became normal, and arterial blood pressure, heart rate, and S_pO_2 were also monitored (by M1020 module, Hewlett-Packard). Figure 11.5 shows mean COHb values with corresponding S_pO_2 levels.

For all 18 measurements, the mean S_pO_2 reading was above 91%, which would be readily accepted as sufficient oxygenation. Decrease in COHb concentrations led to a slight increase of S_pO_2, as would be expected by the formula (Tremper and Baker 1989)

$$S_pO_2 = \frac{(c_{HbO_2} + 0.9c_{COHb})}{c_{\text{total hemoglobins}}} \times 100\%. \qquad (11.4)$$

As the level of COHb concentration in the blood reduces, the concentration of HbO_2 will rise while the concentration of total hemoglobins remain the same. Therefore, the magnitude of the numerator ($c_{HbO_2} + 0.9c_{COHb}$) of equation (11.4) will increase which results in a larger $S_pO_2$value.

MASIMO 2053
Apple v. Masimo
IPR2022-01300
APL_MAS_ITC_00015821
RX-0035.0204

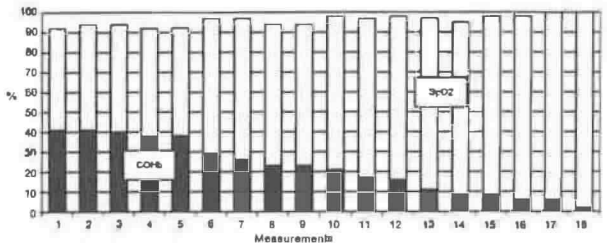

Figure 11.5 Mean measured arterial blood oxygen saturation (S_pO_2) with corresponding COHb values for 18 measurements in 6 patients. From Seidler (1993).

The increasing availability of pulse oximetry in intensive care units may lead to a false interpretation of oxygen transport capacity in cases of CO poisoning, especially if S_pO_2 is between 91% and 98%. Physicians should be aware that the diagnosis of CO poisoning still depends on a high degree of clinical suspicion and direct measurement of CO (Seidler *et al* 1993). The normal level of COHb in the arterial blood is less than 2%. Smokers or smoke-inhalation victims may have COHb levels greater than 10%. A high level of COHb overestimates the S_aO_2 values.

11.7.2 Methemoglobin (MetHb)

Methemoglobin is hemoglobin with iron oxidized from the normal (or reduced) ferrous (Fe^{2+}) state to the ferric (Fe^{3+}) state as described earlier in chapter 4. Methemoglobin is incapable of transporting oxygen.

Methemoglobinemia (high level of MetHb present in the blood) may be induced by a large number of drugs including local anesthetics (prilocaine, benzocaine), nitrates (nitroglycerin), nitrites, phenacetin, pyridium, primiquine, and sulfonamides. There are several case reports of potentially serious methemoglobin levels (greater than 30%) induced by topical anesthetics used in the airway. There are also case reports describing pulse oximeter readings during methemoglobinemia. However, the MetHb levels in these were too low (6% or less) to accurately characterize pulse oximeter behaviour.

At 660 nm the extinction coefficient of MetHb is similar to that of Hb and much greater than that of HbO_2 (figure 4.2). At 940 nm MetHb has a greater extinction coefficient than either Hb or HbO_2. MetHb thus adds to the pulse additional absorbance at both wavelengths. In contrast, COHb adds significant absorbance only at the shorter wavelength, where COHb has an extinction coefficient comparable to that of HbO_2. S_pO_2 is computed from the ratio R of the pulse-added absorbances at the two wavelengths. The presence of MetHb increases both the numerator and denominator of this ratio, which tends to drive R toward unity.

The arterial oxygen saturation can be expressed as

$$S_pO_2 = HbO_2\,\% = \frac{c_{HbO_2}}{c_{\text{total hemoglobins}}} \times 100\% \qquad (11.5)$$

MASIMO 2053
Apple v. Masimo
IPR2022-01300
APL_MAS_ITC_00015822
RX-0035.0205

while the functional hemoglobin saturation (measured arterial saturation)

$$S_pO_2 = \frac{c_{HbO_2}}{c_{Hb} + c_{HbO_2}} \times 100\% \tag{11.6}$$

$$= \frac{c_{HbO_2}}{c_{\text{total hemoglobins}} - c_{MetHb} - c_{COHb}} \times 100\%. \tag{11.7}$$

Theoretically, from equations (11.5) and (11.7), we can see that in the presence of MetHb, pulse oximeters overestimate the value of oxygen saturation in arterial blood, i.e., S_pO_2 is greater than S_aO_2.

11.7.3 Fetal hemoglobin

One of the concerns clinicians often have related to the interpretation of pulse oximeter readings in newborn infants is the fetal hemoglobin (HbF) present in the blood because pulse oximeters are calibrated empirically by inducing hypoxia in healthy adults. At birth, newborns have approximately 60 to 95% of the total hemoglobin in the form of fetal hemoglobin while the remainder is adult hemoglobin (HbA). In infants older than nine months, HbF levels higher than 2% often indicate an anemia such as sickle-cell anemia.

Mendelson and Kent (1989), and Zijlstra *et al* (1991) demonstrated that there is no significance difference in absorption spectra of adult and fetal hemolyzed blood in the 650 to 1000 nm wavelength region, which is used in pulse oximetry. On the other hand, adult and fetal hemoglobin absorption characteristics differ in the range of wavelengths below 650 nm.

The theoretical S_pO_2 readings for the adult and fetal hemoglobin can be determined by substituting the extinction coefficients given in table 11.6 into equation (4.19), which is

$$S_aO_2 = \frac{\varepsilon_{Hb}(\lambda_R) - \varepsilon_{Hb}(\lambda_{IR})R}{\varepsilon_{Hb}(\lambda_R) - \varepsilon_{HbO_2}(\lambda_R) + [\varepsilon_{HbO_2}(\lambda_{IR}) - \varepsilon_{Hb}(\lambda_{IR})]R} \times 100\%. \tag{11.8}$$

Table 11.6 Extinction coefficients of adult and fetal blood expressed in ($L \cdot mmol^{-1} \cdot cm^{-1}$) (from Mendelson and Kent 1991).

	Hb		HbO_2	
λ	Adult	Fetal	Adult	Fetal
660 nm	0.86	0.90	0.12	0.16
940 nm	0.20	0.20	0.29	0.30

Figure 11.6 shows the results of the theoretical simulation. Mendelson and Kent (1989) suggested that a maximum error of approximately 3% in pulse oximeter oxygen saturation readings could be expected when measurements from adult and fetal blood are compared.

MASIMO 2053
Apple v. Masimo
IPR2022-01300
APL_MAS_ITC_00015823
RX-0035.0206

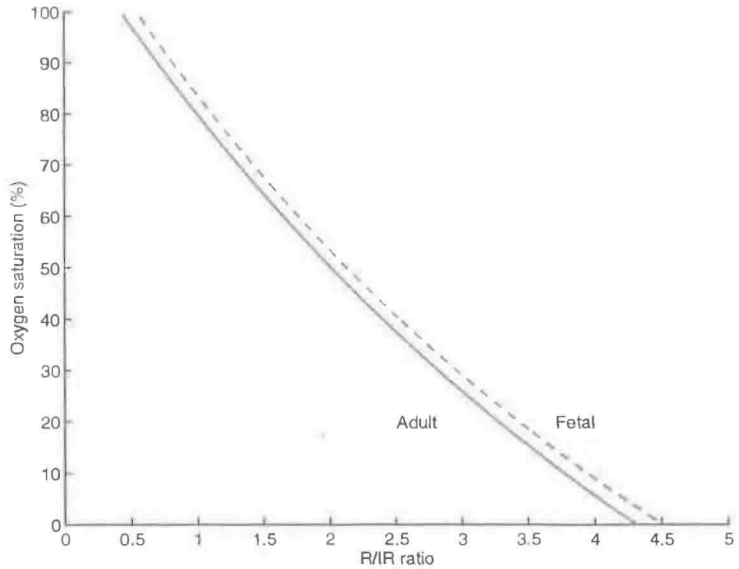

Figure 11.6 The calibration curves derived from a theoretical simulation show that pulse oximeters will read about 3% high for fetal hemoglobin. The R/IR ratio is R in equation (11.6).

11.7.4 Bilirubin

Bilirubin is an orange or yellow colored compound which is a breakdown product of heme. High levels of bilirubin can affect absorbance at lower wavelengths used by the CO-oximeters. A bilirubin concentration of 20 mg/dl will cause up to 1% error in the measurement of four main hemoglobin species. The absorption spectrum of bilirubin has a peak at 460 nm and much smaller peaks at 560 and 600 nm. Veyckemans *et al* (1989) showed that there was no significant error detected from the influence of high bilirubin plasma levels. The presence of bilirubin in the arterial blood will not induce any significant errors in pulse oximetry measurements.

11.8 EFFECT OF TEMPERATURE

11.8.1 Ambient temperature

An exposure of the body to cold temperatures can cause changes in peripheral perfusion which may cause inaccuracy. The temperature dependence of LEDs in pulse oximeter probes is unlikely to affect the pulse oximetric values. Reynolds *et al* (1991) showed that there was a 5.5 nm increase in the peak wavelength for a 660 nm LED, and a 7.8 nm increase in the peak wavelength for a 950 nm LED as temperature increased from 0 to 50 °C (see chapter 10).

MASIMO 2053
Apple v. Masimo
IPR2022-01300
APL_MAS_ITC_00015824
RX-0035.0207

Table 11.7 Extinction coefficients at 0 °C and 50 °C expressed in (L mmol^{-1} cm^{-1}). Adapted from Reynolds *et al* (1991).

	Hb		HbO_2	
λ	0 °C	50 °C	0 °C	50 °C
660 nm	0.856	0.811	0.123	0.117
950 nm	0.153	0.139	0.274	0.265

Table 11.7 lists the extinction coefficients of Hb and HbO_2 at different wavelengths and temperatures. Substituting these values into the relationship between S_pO_2 and R given in equation (11.6) which is derived from Beer's law, theoretical calibration curves can be obtained as in figure 11.7. Thus the effect of shifts in wavelength of the LEDs on pulse oximeter accuracy is neglibible as the temperature increases from 0 °C to 50 °C.

The reduced amplitude of the ac signals occurring during cold exposure causes the pulse oximeter to be more sensitive to motion artifacts, for example those caused by shivering or coughing. These artifacts may cause the pulse oximeter to give an erroneous value of S_pO_2. Reynold *et al* (1991) concluded that inaccuracies in pulse oximeter readings at extreme temperatures are far more likely to be caused by reductions in peripheral perfusion, rather than a result of the temperature dependence of the LEDs in the pulse oximeter probe.

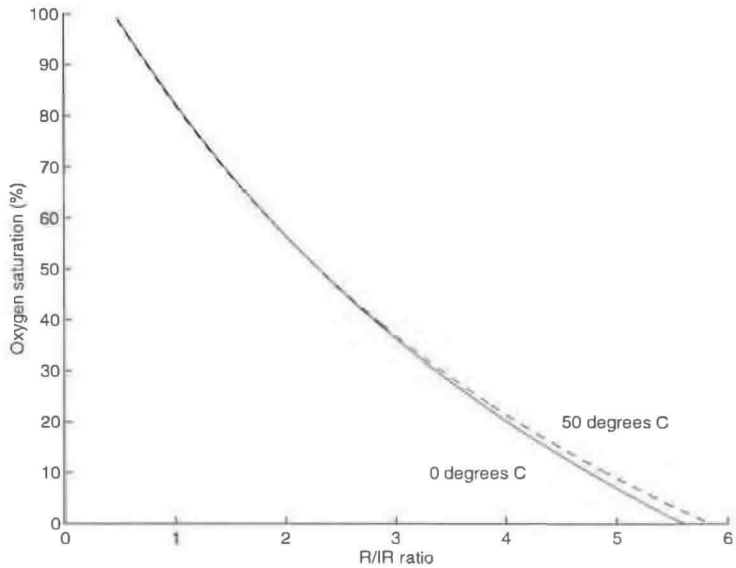

Figure 11.7 The calibration curves from a theoretical model show a shift from 0 °C to 50 °C.

11.8.2 Patient temperature

Errors in pulse oximetry readings do not increase significantly with a decrease in patient temperature. Palve and Vuori (1989) found that, in a recovery room

MASIMO 2053
Apple v. Masimo
IPR2022-01300
APL_MAS_ITC_00015825
RX-0035.0208

study of the Nellcor N-100 and Ohmeda Biox 3700 pulse oximeters, they were reliable on patients with low cardiac output and hypothermia after open heart surgery, with standard deviations ranging from 1.8% to 3.9% for finger probes and from 0.9% to 2.1% for ear probes which are comparable to the outcomes of normal cases.

11.9 ACCURACY VERSUS MEDICAL CONDITIONS

Although pulse oximeters are designed to help detect pathophysiological oxygenation conditions of patients that might lead to a life threatening situation, some medical conditions cause pulse oximeters to be unreliable. Fortunately, pulse oximetry works well in the majority of the cases. The following are some frequent encounters where the accuracy of pulse oximeters is often questioned.

11.9.1 Cardiac arrhythmia

The heart rate derived from a pulse oximeter should match that from an ECG signal for the patient with a healthy heart. If the two differ, either of the monitors may be in error because of poor signal quality, or the electrical activity of the heart may appear to be normal while it produces beats with inadequate stroke volume output due to inadequate filling or contraction (Webb *et al* 1991).

Wong *et al* (1989) conducted an experiment to test the accuracy of pulse oximeters for 163 patients with cardiac arrhythmias. They found that for the group of 24 patients with a pulse oximeter to ECG pulse rate discrepancy of greater than 3 beats/min, S_pO_2 measurements were as accurate as those for the group of 139 patients with pulse rate agreement, as long as the S_pO_2 reading was stable on the pulse oximeter and there was reasonable signal strength.

11.9.2 Myxoma

Fearley and Manners (1993) described a case of inaccurate oximetry in a patient with a right ventricular myxoma. The ventilation/perfusion scan of the patient was normal but cardiac angiography revealed a rounded mass in the right ventricular outflow tract. Before cardiopulmonary bypass, pulse oximetry using an ear probe gave a consistent hemoglobin saturation of 75%, but repeated arterial blood gas analysis showed an arterial oxygen saturation exceeding 95%. The ear probe gave readings of 96 to 98% on volunteers in the operating room. Postoperative oximetry was consistently more than 96%. It was concluded that a ventricular contribution to the central venous pressure due to the dilated tricuspid ring might lead to the inaccuracy in pulse oximetry. The pulsatile venous pressure presumably induced an alternating current in the oximeter giving rise to a saturation not related to the arterial oxygen saturation. Thus pulse oximeter readings must be interpreted carefully in the clinical context of the patient being monitored.

11.10 ACCURACY VERSUS PROBE POSITION

Severinghaus *et al* (1989) found that ear and forehead probes generally had a much faster response to changing S_pO_2 values than finger probes. It was

MASIMO 2053
Apple v. Masimo
IPR2022-01300
APL_MAS_ITC_00015826
RX-0035.0209

suggested that finger probes require a greater transit time for blood to reach the finger compared to ear. Kagle *et al* (1987) found the Ohmeda 3700 finger probe to be on average 24 s behind the Ohmeda 3700 ear probe in its response to rapid desaturation. West *et al* (1987) found that measurement accuracy was related to response delay times, with longer delays associated with lower accuracy. The ear probe with the shortest delay had some accuracy problems at low saturations, and the slowest responding finger probe was claimed to be totally inadequate as a monitor of rapid changes in saturation due to its delayed and highly damped response.

Forehead probes have been tested at stable low saturations on volunteers by Cheung and Stommel (1989) using a commercially available unit and Mendelson *et al* (1988) using a custom-built reflectance probe. Both groups found good correlation between the forehead measured values and CO-oximetry measurements for saturations down to 65%. Severinghaus *et al* (1989) found the accuracy of seven forehead probes to be comparable to that of finger probes during rapidly induced desaturation in volunteers.

Table 11.8 Accuracy of pulse oximeters ranked according to percentage of readings within 3% of the CO-oximeter readings out of the total number of readings. From Clayton *et al* (1991b).

Pulse oximeter	Total	# within ±3%	Percent ±3%/Total	Rank
Criticare CSI 503 finger	40	40	100	1
Datex Satlite finger	40	38	95	2
Criticare CSI 503 ear	17	16	94	3
Novametrix 505 finger	38	35	92	4
Criticare CSI 504 finger	39	35	90	5
Datex Satlite ear	35	31	89	6
Physio-Control 1600 ear	36	32	89	6
Invivo 4500 finger	38	34	89	6
Radiometer Oximeter ear	36	32	89	6
Sensormedics Oxyshuttle finger	36	32	89	6
Ohmeda Biox 3740 finger	28	26	87	11
Criticare CSI 504 ear	14	12	86	12
Physio-Control 1600 finger	36	31	86	12
Sensormedics Oxyshuttle ear	35	30	86	12
Radiometer Oximeter finger	40	32	80	15
Ohmeda Biox 3700 ear	40	30	75	16
Ohmeda Biox 3740 ear	34	25	74	17
Ohmeda Biox 3700 finger	36	25	69	18
Datex Satlite forehead	37	22	59	19
Novamatrix 505 nose	34	19	56	20
Invivo 4500 nose	26	8	31	21

Under poor perfusion conditions, pulse oximeters might either fail to provide a reading or give a '***Low signal quality***' warning. Clayton *et al* (1991b) studied the performance of probes under conditions of poor peripheral perfusion in patients who have undergone cardiopulmonary bypass in the immediate postoperative period. The results are shown in table 11.8. Finger probes were to found to have better performances than the ear, nose, and forehead probes and the authors recommended using them during poor perfusion situations. It was also noted that ear probes generally had the faster response as reported by other studies (Severinghaus *et al* 1989, West *et al* 1987, Kagle *et al* 1987). The delay of finger probes should be taken into account when planning critical management algorithms.

MASIMO 2053
Apple v. Masimo APL_MAS_ITC_00015827
IPR2022-01300
RX-0035.0210

11.11 ELECTROMAGNETIC INTERFERENCE

Electromagnetic interference (EMI) includes several different sources of interference from the electromagnetic spectrum. It may be generated by many sources, mostly man made but also results from atmospheric events and cosmic noise. Even nuclear explosions produce an enormous electromagnetic pulse interference. All electronic devices are affected by EMI, but the consequences are more serious when affecting medical devices such as pacemakers and pulse oximeters. Frequent sources of interference are electrostatically charged operators, communications transmissions, other medical devices, and other electrical and electronic equipment.

Pulse oximeters contain a microprocessor and many other electronic circuits that are very sensitive to EMI. The requirement in their design for a high degree of electromagnetic compatibility (EMC) is now required by statute, such as the Food and Drug Administration (FDA) in the United States. The Center for Devices and Radiological Health (CDRH) is developing a comprehensive strategy of EMC requirements for medical devices.

A performance degradation in pulse oximetry due to radiated interference was reported by Silberberg (1996). A pulse oximeter displayed a hemoglobin saturation level of 100% and a pulse rate of 60 for a patient who had deceased earlier that day. This anomalous performance was because a telemetry transceiver had been placed too close to the pulse oximeter. Thus, EMI can contribute a large error to pulse oximetry. Care should be taken to make sure that there is no significance presence of EMI in the environment.

11.11.1 Interference from magnetic resonance imaging (MRI)

The radio frequency transmissions from the magnet and rapidly switching magnetic field gradients are two majors sources of artifact generated in medical devices during magnetic resonance imaging (MRI).

The magnetic resonance scanner places unusual demands on the equipment and practices of patients' safety. As sedation or anesthesia is necessary for successful MRI of some patients (particularly infants and young children), reliable patient monitoring is essential. The strong magnetic field, radio frequency (RF) radiation, and reduced patient access complicate traditional methods of patient monitoring. Conventional ECG monitoring, for instance, is subject to artifactual changes during MRI. Moreover, infants have smaller oxygen reserves which, coupled with their higher metabolic rate, can lead to rapid decreases in blood oxygenation S_pO_2. Pulse oximetry is ideal to use during MRI. It is flexible as to the choice of monitoring site, and suffers few problems from induced electromagnetic noise.

The difficulties in using pulse oximetry in MRI stem largely from the design of the monitor unit. Pulse oximeters adapted to the MRI environment have a compact nonmetallic housing and are battery operated. Extended fiber optic leads are also used to keep the electronics outside the bore of the MRI magnet as described in chapter 7. Because there are no electric cables extending through the magnetic resonance imager bore, there is no possibility of RF burns to the patient or RF-induced noise in the signal conveyed to the processor and display unit. However, the fiber optic leads tend to be relatively delicate and easily broken. Once damaged, the cost of repair is very high. Furthermore, fiber optic systems

MASIMO 2053
Apple v. Masimo
IPR2022-01300
APL_MAS_ITC_00015828
RX-0035.0211

normally require different probes for patients of different size, particularly separate adult and pediatric probes. Individual probes are very expensive.

Blakeley *et al* (1994) proposed a design system for a MRI-compatible pulse oximeter which is shown in figure 11.8. The radio frequency signals can be eliminated by using notch filters and a low-pass filter. This system can prevent radio frequency burns in patients. The proposed system also worked with existing pulse oximeters. No modifications of pulse oximeters are needed.

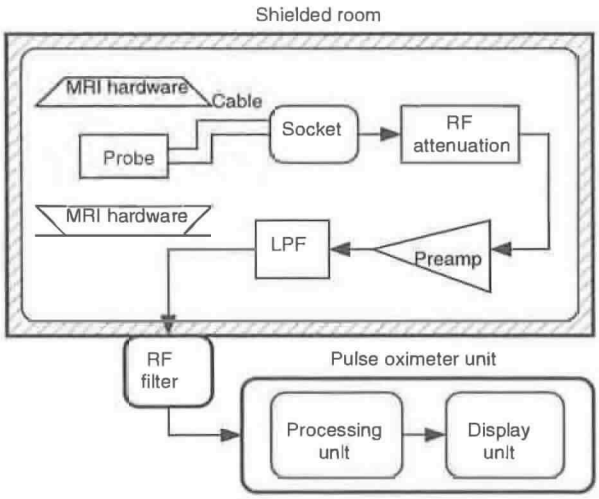

Figure 11.8 MRI compatible pulse oximetry (adapted from Blakeley *et al* 1994).

11.12 OTHER EFFECTS ON ACCURACY

Besides the major sources of errors described in previous sections, users frequently encounter other circumstances where the accuracy of a pulse oximeter is questioned. The followings are some factors which have some effects on the performance of a pulse oximeter, although no large error is expected.

11.12.1 Exercise

The presence of cardiorespiratory abnormalities during physical stress may not be noticeable under resting conditions. These abnormalities can be investigated by exercise stress testing which requires the pulse oximetry technique (see section 13.6.2). Powers *et al* (1989) and Williams *et al* (1986) found that pulse oximeters using ear probes underestimated arterial saturation by 10 to 15% during heavy exercise. It was suggested that this is caused by reduced ear perfusion in exercise. Smyth *et al* (1986) in contrast found up to 15% overestimation by a pulse oximeter using an ear probe during exercise under hypoxic conditions.

In a more recent study by Norton *et al* (1992), 10 subjects were used to perform strenuous exercise on a bicycle ergometer. Blood oxygen saturations

MASIMO 2053
Apple v. Masimo
IPR2022-01300
APL_MAS_ITC_00015829
RX-0035.0212

were measured using the Ohmeda Biox pulse oximeter 3700R with the ear probe, and the blood gas analyzer (Ciba-Corning, model 278). The results of oxygen saturation levels obtained indicated that relatively large underestimations of S_aO_2 can occur when a pulse oximeter is used, and these errors increase as the severity of exercise increases. Powers *et al* (1989) found similar results. Further studies are still needed to investigate the performance of pulse oximeters during exercise. Estimations of arterial blood oxygen saturation during severe exercise using the pulse oximetry technique should be viewed with caution, as potentially large errors may occur.

11.12.2 Dried blood

Trauma patients may have significant quantities of dried blood remaining on their hands upon arrival in the emergency department. There is often insufficient time to clean the patient's hand thoroughly before the application of the pulse oximeter probe (Rosewarne and Reynolds 1991). In a study by Rosewarne and Reynolds (1991), the finger probes of six commercially available pulse oximeters were applied to the fingers of a healthy male Caucasian volunteer. Two of the fingers had previously been coated in whole blood which was allowed to dry. Rosewarne and Reynolds (1991) found that there was no significant difference in saturation range among those fingers with or without dried blood. The variation in readings between brands of pulse oximeter was of the same order as between fingers.

In emergency situations, the presence of dried blood is unlikely to cause a decline in pulse oximeter accuracy and performance as long as adequate perfusion is maintained.

11.12.3 Pigments

In theory, skin pigmentation and other surface light absorbers such as nail polish, should not cause errors in S_pO_2 readings since the pigments absorb a constant fraction of the incident light, and the pulse oximeters use only pulsatile absorption data. The absorbances of light by the pigments are nonpulsatile and, just as for tissue absorption, are cancelled out of the saturation calculation.

However, Cote *et al* (1988) found that black, blue, and green nail polishes caused a significant lowering of S_pO_2 readings of the Nellcor N-100, while red and purple nail polish did not. Cecil *et al* (1988) also showed apparently greater inaccuracy in pulse oximeter readings for black patients. This is probably caused by the fact that N-100 increases its light output in response to low detected light levels, and the higher LED current caused a shift in the output spectrum (see chapter 5). The shifting of the peak wavelength of LEDs affects the measured transmitted red and infrared light intensities, and thus alters the oxygen saturation reading. For the nail polish problem, the solution is to mount the probe side-to-side on the finger (White and Boyle 1989). This technique may also help to avoid the saturation underestimation problem caused by only partial placement of the LEDs over the finger because of very long fingernails.

REFERENCES

Blakeley D G, Gauss R C and Flugan D C 1994 MRI compatible pulse oximetry *US patent: 5,323,776*

MASIMO 2053
Apple v. Masimo APL_MAS_ITC_00015830
IPR2022-01300
RX-0035.0213

Cahan C, Decker M J, Hoekje P L and Strohl K P 1990 Agreement between noninvasive oximetric values for oxygen saturation *Chest* **97** 814–9
Casciani J R, Mannheimer P D, Nierlich S L and Ruskewicz S J 1995 Pulse oximeter sensor optimized for low saturation *US patent 5,421,329*
Cecil W T, Thorpe K J, Fibuch E E and Tuohy G F 1988 A clinical evaluation of the accuracy of the Nellcor N-100 and the Ohmeda 3700 pulse oximeters *J. Clin. Monit.* **4** 31–6
Cheung E Y and Stommel K A 1989 Quantitative evaluation of a combined pulse oximetry and end-tidal CO_2 monitor *Biomed. Instrum. Technol.* **23** 216–21
Choe H, Tashiro C, Fukumitsu K, Masahuru Y and Yoshiya I 1989 Comparison of recorded values from six pulse oximeters *Crit. Care Med.* **17** 678–81
Clayton D G, Webb R K, Ralston A C, Duthie D and Runciman W B 1991a A comparison of the performance of 20 pulse oximeters under conditions of poor perfusion *Anaesthesia* **46** 3–10
Clayton D G, Webb R K, Ralston A C, Duthie D and Runciman W B 1991b Pulse oximeter probe: A comparison between finger, nose, ear and forehead probes under conditions of poor perfusion *Anaesthesia* **46** 260–5
Cote C J, Goldstein E A, Fuchsman W H and Hoaglin D C 1988 The effect of nail polish on pulse oximetry *Anesth. Analg.* **67** 683–6
ECRI 1989 Pulse oximeters *Health Devices* **18** 185–230
Fearley S J and Manners J M 1993 Pulse oximetry artefact in a patient with a right atrial myxoma *Anaesthesia* **48** 87–8
Kagle D M, Alexander C M, Berko R S, Giuffre M and Gross J B 1987 Evaluation of the Ohmeda 3700 pulse oximeter: steady-state and transient response characteristics *Anesthesiology* **66** 376–80
Mendelson Y, Kent J C, Yocum B L and Birle M J 1988 Design and evaluation of a new reflectance pulse oximeter sensor *Med. Instrum.* **22** 167–73
Mendelson Y and Kent J C 1989 Variations in optical absorption spectra of adult and fetal hemoglobins and its effect on pulse oximetry *IEEE Trans. Biomed. Eng.* **36** 844–8
Nickerson B G, Sarkisian C and Tremper K 1988 Bias and precision of pulse oximeters and arterial oximeters *Chest* **93** 515–7
Norton L H, Squires B, Craig N P, McLeay G, McGrath P and Norton K I 1992 Accuracy of pulse oximetry during exercise stress testing *Int. J. Sports Med.* **13** 523–7
Palve H and Vuori A 1989 Pulse oximetry during low cardiac output and hypothermia states immediately after open heart surgery *Crit. Care Med.* **17** 66–9
Powers S K, Dodd S, Freeman J, Ayers G D, Samson H and McKnight T 1989 Accuracy of pulse oximetry to estimate HbO_2 fraction of total Hb during exercise *J. Appl. Physiol.* **67** 300–4
Reynolds K J, de Kock J P, Tarassenko L and Moyle J T B 1991 Temperature dependence of LED and its theoretical effect on pulse oximetry *Br. J. Anaesth.* **67** 638–43
Rosewarne F A and Reynolds K J 1991 Dried blood does not affect pulse oximetry *Anaesthesia* **46** 886–70
Saito S, Fukura H, Shimada H and Fujita T 1995 Prolonged interference of blue dye "patent blue" with pulse oximetry readings *Acta Anaesthesiol. Scand.* **39** 268–9
Scheller M S, Unger R J and Kelner M J 1986 Effects of intravenously administered dyes on pulse oximetry readings *Anesthesiology* **65** 550–2
Seidler D, Hirschl M M and Roeggla G 1993 Limitations of pulse oximetry *Lancet* **341** 1600–1
Severinghaus J W, Naifeh K H and Koh S O 1989 Errors in 14 pulse oximeters during profound hypoxia *J. Clin. Monit.* **5** 72–81
Siegel M N and Gravenstein N 1987 Preventing ambient light from affecting pulse oximetry *Anesthesiology* **67** 280
Silberberg J L 1996 Electronic medical devices and EMI *Compliance Eng.* **XIII** (2) D14–21
Smyth R J, D'urzo A D, Slutsky A S, Galko B M and Rebuck A S 1986 Ear oximetry during combined hypoxia and exercise *J. Appl. Physiol.* **60** 716–9
Taylor M B and Whitwam J G 1988 The accuracy of pulse oximeters: a comparative clinical evaluation of five pulse oximeters *Anaesthesia* **43** 229–32
Tremper K K and Barker S J 1989 Pulse oximetry *Anesthesiology* **70** 98–108
Veyckemans F, Baele P, Guillaume J E, Willems E, Robert A and Clerbaux T 1989 Hyperbilirubinemia does not interfere with hemoglobin saturation measured by pulse oximetry *Anesthesiology* **70** 118–22
Webb R K, Ralston A C and Runciman W B 1991 Potential errors in pulse oximetry, II. Effects of changes in saturation and signal quality *Anaesthesia* **46** 207–12
West P, George C F and Kryger M H 1987 Dynamic *in vivo* response characteristics of three oximeters. Hewlett-Packard 47201A, Biox III, and Nellcor N-100 *Sleep* **10** 263–71
White P F and Boyle W A 1989 Nail polish and oximetry *Anesth. Analg.* **68** 546–7

MASIMO 2053
Apple v. Masimo APL_MAS_ITC_00015831
IPR2022-01300
RX-0035.0214

Williams J, Powers S and Stuart M 1986 Hemoglobin desaturation in highly trained endurance athletes during heavy exercise *Med. Sci. Sports Exercise* **18** 168–73
Wong D H, Tremper K K, Davidson J, Zaccari J, Weidoff P, Wilbur S and Stemmer E A 1989 Pulse oximetry is accurate in patients with dysrhythmias and a pulse deficit *Anesthesiology* **70** 1024–5
Yelderman M and New W 1983 Evaluation of pulse oximetry *Anesthesiology* **59** 349–52
Zijlstra W G, Buursma A and Meeuwsen-van der Roest W P 1991 Absorption spectra of human fetal and adult oxyhemoglobin, de-oxyhemoglobin, carboxyhemoglobin, and methemoglobin *Clin. Chem.* **37** 1633–8

INSTRUCTIONAL OBJECTIVES

11.1 Explain the differences between between bias, precision, and the 95% confidence limit.
11.2 Describe the accuracy of pulse oximeters in the three ranges of oxygen saturation levels.
11.3 Using the absorption spectra shown in figure 11.1, explain why the accuracy is worse at low oxygen saturation level.
11.4 Describe the accuracy of pulse oximeters at low perfusion and how to prevent the errors.
11.5 Explain how venous congestion occurs and its results on pulse oximeter accuracy.
11.6 Describe two sources of optical intereferences and their effects on pulse oximeter accuracy.
11.7 Describe how to prevent errors from high intensity ambient light.
11.8 Describe how the absorbance of dyes affects the accuracy of pulse oximeters.
11.9 Explain the effects of MeBl on pulse oximeter readings.
11.10 Given c_{HbO_2} and c_{COHb}, calculate the estimated S_pO_2
11.11 Describe how MetHb and bilirubin affect the readings of pulse oximeters.
11.12 Describe how fetal hemoglobin affects the readings of pulse oximeters.
11.13 Explain how temperature affects pulse oximeter accuracy and describe how the theoretical calibration curve shifts from 0 °C to 50 °C.
11.14 Describe the accuracy and response time of finger probes and ear probes during rapid desaturation and low perfusion.
11.15 Explain the effect of EMI on pulse oximeter accuracy.
11.16 Describe the effect of MRI on pulse oximetry and explain the system of MRI-compatible pulse oximetry.
11.17 Describe the effect of pigments on the accuracy of pulse oximeters.

MASIMO 2053
Apple v. Masimo
IPR2022-01300
APL_MAS_ITC_00015832
RX-0035.0215

CHAPTER 12

USER INTERFACE FOR A PULSE OXIMETER

Albert Lozano-Nieto

12.1 INTRODUCTION

This chapter deals with some important aspects that need to be considered when designing any kind of product whose final goal is to be marketed rather than be used as a laboratory prototype. The product has to be built so that it will solve a need for the customer. A product that is technologically perfect can result in an economic failure if it is not sold because it does not meet the user's expectations or needs, it is not sold because it is too complicated to operate, or is removed from the market by the regulatory agencies because it does not meet the applicable regulations.

This chapter will highlight those aspects of the overall design for a pulse oximeter that may not receive enough attention when designing the hardware and software that make up the core of the system. These aspects are the design of an optimal user interface system, so that the final product will comply with all the regulations that apply to that specific product.

The chapter is organized by discussing the options available to the designers for the different stages that form a pulse oximeter, by reviewing how choices have been made in commercially available equipment, and by discussing which standards are applicable to the different parts of the pulse oximeter and their consequences for the design. The standards are a collection of rules, most of them based on common sense, used to ensure the best results in the use of pulse oximeters. In particular, we must comply with the *Standard Specifications for Pulse Oximeters, F1415-1992* from the American Society for Testing and Materials (ASTM) that compiles the current regulations for the design of pulse oximeters (ASTM 1992). This Standard references the *Safety of Medical Electrical Equipment—Part 1, General Safety Requirements, IEC 601-1* standard from the International Electrical Commission (IEC) for many general requirements concerning safety, and discusses the specific variations from the IEC 601-1 in the case of pulse oximeters (IEC 1988). A more detailed discussion about some aspects of the IEC 601-1 Standard for pulse oximeters is in the ISO 9919 Standard, *Pulse Oximeters for medical use—Requirements* (IOS 1992). Nevertheless, all the standards are subjected to revision, and undergo changes with the development of technology and other standards that affect related

MASIMO 2053
Apple v. Masimo
IPR2022-01300
APL_MAS_ITC_00015833
RX-0035.0216

equipment. For example, in 1996, development began on a standard that will apply to all medical devices used during anesthesia. So, it is the responsibility of the designer to know and comply with the current applicable standards.

12.2 FRONT PANEL

The front panel of a pulse oximeter communicates between the patient and the healthcare professionals. This communication is expected to be accurate and clear. The accuracy problems are related to the core design, discussed in the previous chapters. This chapter will focus on how to make this communication as effective as possible, designing the pulse oximeter to display the necessary information in the way that is most useful to healthcare professionals.

Figure 12.1 shows how to model a pulse oximeter as a transducing system that transforms a variable from the chemical domain (arterial oxygen saturation), to a variable in the electrical domain that can be further processed, stored or displayed. While previous chapters have treated the first conversion stages, we will discuss the last conversion stages, that is, how the information is presented to the operator.

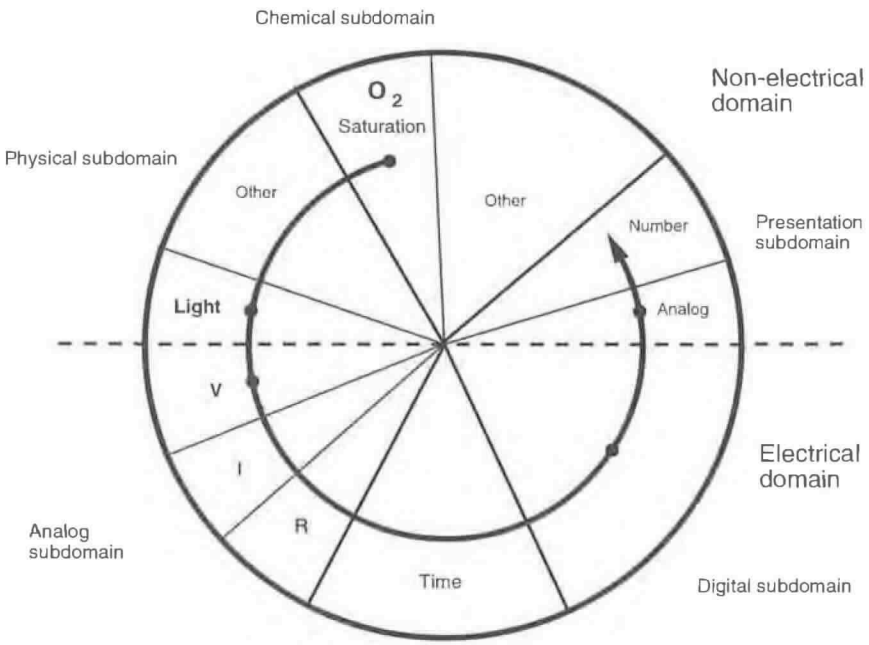

Figure 12.1 Change of domains of information in a pulse oximeter. Adapted from Malmstad *et al* (1973).

We will consider two main ways of presenting information to a human operator. These are visually and acoustically. The acoustic way is mainly used to alert the operator of a possible malfunction of the monitoring equipment or a medical

MASIMO 2053
Apple v. Masimo
IPR2022-01300
APL_MAS_ITC_00015834
RX-0035.0217